

FEDFA: FEDERATED LEARNING WITH FEATURE ANCHORS TO ALIGN FEATURE AND CLASSIFIER FOR HETEROGENEOUS DATA

Tailin Zhou¹, Jun Zhang¹ & Danny Tsang^{2,1}

The Hong Kong University of Science and Technology¹

HongKong, China

The Hong Kong University of Science and Technology (Guangzhou)²

Guangzhou, Guangdong, China

{tailin.zhou, eejzhang, eetsang}@ust.hk

ABSTRACT

Federated learning allows multiple clients to collaboratively train a model without exchanging their data, thus preserving data privacy. Unfortunately, it suffers significant performance degradation under heterogeneous data at clients. Common solutions in local training involve designing a specific auxiliary loss to regularize weight divergence or feature inconsistency. However, we discover that these approaches fall short of the expected performance because they ignore the existence of a *vicious cycle* between classifier divergence and feature mapping inconsistency across clients, such that client models are updated in inconsistent feature space with diverged classifiers. We then propose a simple yet effective framework named **Federated learning with Feature Anchors** (FedFA) to align the feature mappings and calibrate classifiers across clients during local training, which allows client models updating in a shared feature space with consistent classifiers. We demonstrate that this modification brings similar classifiers and a *virtuous cycle* between feature consistency and classifier similarity across clients. Extensive experiments show that FedFA significantly outperforms the state-of-the-art federated learning algorithms on various image classification datasets under label and feature distribution skews.

1 INTRODUCTION

With massive data located at edge clients of large-scale networks like the internet of things networks, federated learning (McMahan et al., 2017) enables clients to jointly train a machine learning model without collecting client data into a centralized server, thus preserving data privacy. However, the private data are typically heterogeneous across clients, resulting in slower convergence (Li et al., 2020; Karimireddy et al., 2020) and degraded generalization performance (Zhao et al., 2018; Li et al., 2021a). This is because data heterogeneity makes the local objectives inconsistent with the global objective and thus the converged model deviates from the expected optima (Wang et al., 2020b).

Common works improve local optimization by controlling weight divergence and feature inconsistency to address the data heterogeneity issue at client side. Client-side methods involve adding a regularizer to control weight divergence such as (Li et al., 2020; Acar et al., 2021) or feature inconsistency across clients such as (Li et al., 2021b; Zhang et al., 2021). Nevertheless, recent works (Li et al., 2021a; Chen & Chao, 2022; Luo et al., 2021) found that these methods did not show clear advantages over the canonical method FedAvg (McMahan et al., 2017) on classification tasks.

Data heterogeneity causes a *vicious cycle* between feature inconsistency and classifier divergence. To unravel the underlying reasons for the ineffectiveness of existing methods, we first observe that data heterogeneity (including heterogeneous label and feature distributions across clients) can induce feature inconsistency and classifier divergence concurrently across clients. We theoretically and empirically identify the existence of a *vicious cycle* between feature inconsistency and classifier divergence across clients, as shown in Figure 1(a). Specifically, inconsistent features diverge the

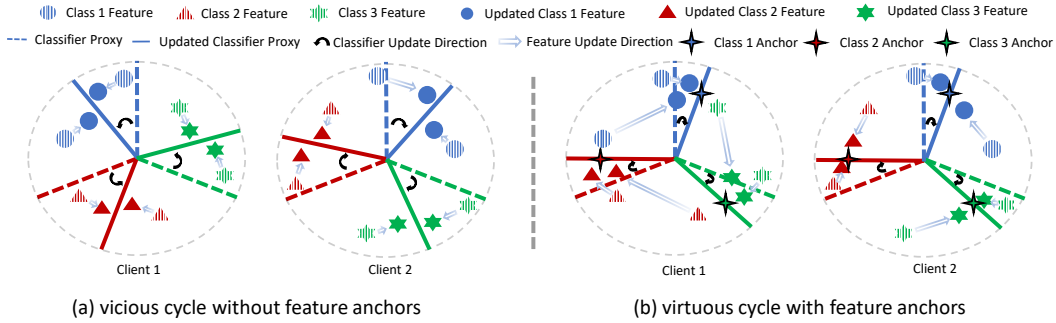


Figure 1: A toy example with three class features to show the rationale of FedFA. Figures 1(a) and 1(b) illustrate the relationship between feature and classifier updates without and with feature anchors, respectively. The *vicious cycle* in Figure 1(a) describes that the diverged classifier updates between client 1 and client 2 due to the inconsistent features (to be verified in Figure 2) make their feature extractors map more inconsistent features to reduce the classification error (i.e., the angle between features and their corresponding classifier proxies) in local training. The *virtuous cycle* in Figure 1(b) means that the aligned features and classifiers by feature anchors between client 1 and client 2 promotes the consistency of client features and classifiers (to be verified in Figure 2).

classifier updates, and then the diverged classifiers force feature extractors to map more inconsistent features, thus diverging client updates.

A new federated learning framework with feature anchors. We propose a simple yet effective framework called *Federated learning with Feature Anchors* (FedFA) for classification tasks to address the skewed label and feature distributions across clients. FedFA introduces the feature anchors to unify the extraction of features by clients from a shared feature space and to calibrate classifier into this space during local training. We show theoretically and empirically that FedFA has a property of similar classifier updates under consistent feature maps, which brings a *virtuous cycle* between classifier similarity and feature consistency as shown in Figure 1(b), contrary to the above *vicious cycle*. Meanwhile, our experiments show that FedFA significantly outperforms the existing methods under label distribution skew, feature distribution skew, and their combined skew. To the best of our knowledge, we are the first to study the combined label and feature distribution skews.

Contributions. The main contributions of this work are summarized as follows:

- We demonstrate how data heterogeneity (i.e., skewed label and feature distributions) lead to a *vicious cycle* between classifier divergence and feature inconsistency across client models.
- To break the *vicious cycle*, we introduce a novel framework FedFA, which leverages feature anchors to aligns features and classifiers across clients such that all client models are updated in a uniform feature space with its corresponding classifiers.
- We proof that FedFA improve the Lipschitzness of the loss on classifier-weight space, which brings a *virtuous cycle* between feature consistency and classifier harmony. Moreover, our experiments show the significant advantage of FedFA over the state-of-the-art algorithms under various data heterogeneity settings.

2 RELATED WORK

Due to space constraints, we mostly introduce approaches most similar to ours (i.e., adding auxiliary loss at client side). Please see Appendix D and E.3 for more detailed discussion.

Tackle data heterogeneity based on weight divergence. To prevent local models from converging to their local minima instead of global minima, many works introduce a weight-space-based regularizer to control local updates. For example, FedProx (Li et al., 2020) uses the Euclidean distance between the local and global models as a regularizer. FedDyn (Acar et al., 2021) modifies the local objective with a dynamic regularizer based on the first-order condition to make clients’ local minima consistent with the global minima. Instead of controlling the divergence of the whole model weights,

(Luo et al., 2021) observes that the classifier layer (i.e., the last layer of the model) suffers most from label distribution skew and calibrates classifier with virtual features after training. Moreover, (Zhang et al., 2022) introduce a fine-grained calibrated classifier loss to prevent the overfitting of missing and minority classes when clients exist the long-tail effect in their dataset.

Tackle data heterogeneity based on feature inconsistency. Some recent works focus more on feature alignment to control feature inconsistency between clients as opposed to regulating weight divergence. For instance, MOON (Li et al., 2021b) introduces a model-contrastive regularizer to maximize (minimize) the agreement of the features extracted by the local model and that by the global model (the local model of the previous round). In place of the model-contrastive term, FedProc (Mu et al., 2021) adds a prototype-contrastive term to regularize the features within each class with class prototypes (Snell et al., 2017). Moreover, FedUFO (Zhang et al., 2021) allows clients to share their own models with other clients to align features and logit output.

Our demonstrations in Section 3 show that current works may still exist feature inconsistency and classifier divergence since these works ignore the relationship between these two issues, as shown in Figures 2 and 5 to 8. Besides, compared with our method, these methods only focus on the performance degeneration under label skewness. In short, by aligning both feature and classifier updates with feature anchors, our work aims to solve the above ignored problem and improve the performance degeneration under both label and feature skewness.

3 INCONSISTENT FEATURES AND DIVERGED CLASSIFIERS ACROSS CLIENTS

3.1 PROBLEM SETUP

Federated learning (McMahan et al., 2017) trains a global model parameterized by vector \mathbf{w} by collaborating a total of N clients with a server to solve the following optimization problem:

$$\min_{\mathbf{w} \in \mathbb{R}^d} \mathcal{L}(\mathbf{w}) := \mathbb{E}_i[\mathcal{L}_i(\mathbf{w})] = \sum_i^N \frac{n_i}{n} \mathcal{L}_i(\mathbf{w}) \quad (1)$$

where $n = \sum_i n_i$ represents the total sample size with n_i being the sample size of the i -th client, and $\mathcal{L}_i(\mathbf{w}) := \mathbb{E}_{\xi \in \mathcal{D}_i} [l_i(\mathbf{w}; \xi)]$ is the local objective function in local dataset \mathcal{D}_i of the i -th client. However, \mathcal{D}_i may differ (i.e., data heterogeneity) between clients such that federated training would not be comparable to centralized training with the global dataset $\mathcal{D} = \cup_i^N \mathcal{D}_i$ (Zhao et al., 2018).

Suppose that the global dataset \mathcal{D} consists of C classes indexed by $[C]$ for classification tasks. Let $(\mathbf{x}, y) \in \mathcal{D}$ and $\mathcal{D} \subseteq \mathcal{X} \times [C]$ where (\mathbf{x}, y) denotes a sample \mathbf{x} in the input-feature space \mathcal{X} with the corresponding label y in the label space $[C]$. We represent $[C_i]$ ($\cup_{i=1}^N [C_i] = [C]$) as a subset of $[C]$ and $\mathcal{D}_{i,c} = \{(\mathbf{x}, c) \in \mathcal{D}_i; c \in [C_i]\}$ as the subset of \mathcal{D}_i with the label c at the i -th client. Moreover, we decompose the classification model parameterized by $\mathbf{w} = \{\theta, \phi\}$ into a *feature extractor* (i.e., other layers except the last layer of the model denoted by $f_\theta : \mathcal{X} \rightarrow \mathcal{H}$) and a *linear classifier* (i.e., the last layer of the model denoted by $f_\phi : \mathcal{H} \rightarrow \mathbb{R}^{[C]}$). Specifically, the feature extractor maps a sample \mathbf{x} into a feature vector $\mathbf{h} = f_\theta(\mathbf{x})$ in the feature space \mathcal{H} , and then the classifier, given the feature \mathbf{h} , generates a probability distribution $f_\phi(\mathbf{h})$ as the prediction for \mathbf{x} . Besides, this work considers both label and feature distribution skews with concrete definitions provided in Appendix A. Briefly, label (feature) distribution skew is the difference of label (input feature) distribution across clients with the same conditional distribution given the label (input feature). It should be noted that the Appendix A has an explanation of all terminology used in this work.

3.2 MOTIVATION: FEATURE INCONSISTENCY AND CLASSIFIER DIVERGENCE

Herein, we visualize the simultaneous occurrence of feature inconsistency and classifier divergence during training and analyse their relationship across clients.

Experimental demonstration. For feature inconsistency, as shown in Figures 2 and 5 to 8, we visualize feature maps of different methods of federated learning under both label and feature distribution skews using t-SNE visualization (Van der Maaten & Hinton, 2008), and also plot the histogram of feature cosine similarity using *positive (negative) pairs* (i.e., features with (without) the same label). For classifier divergence, we input the same samples into all local models to compute the

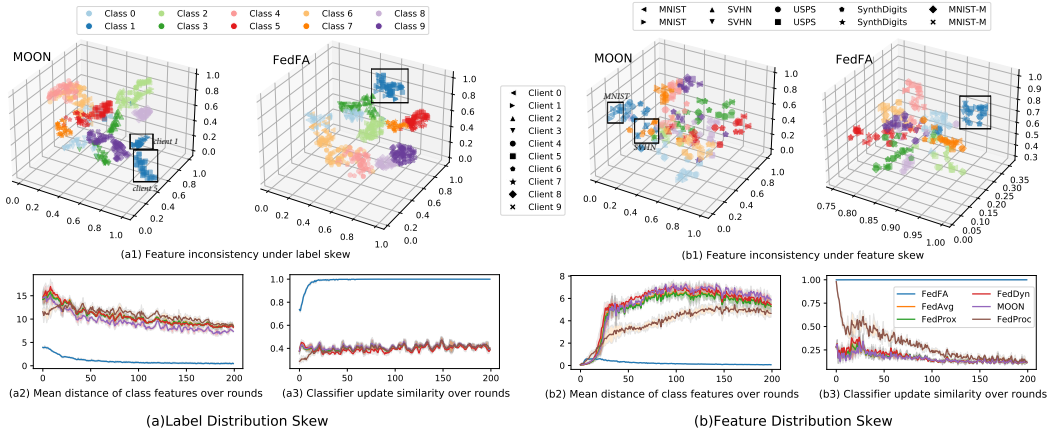


Figure 2: The t-SNE visualization of feature maps, mean distance of class features and classifier update similarity on MOON and FedFA (Our) under label skew ($\#C = 2$) in FMNIST and feature skew in Mixed Digit. Figure 2 reveals the simultaneous occurrence of feature inconsistency and classifier divergence and do not disappear as the global model converges in our baseline methods. Meanwhile, both label and feature skews can induce these two issues, e.g., for class 1 of feature inconsistency (i.e., dark blue), Figure 2(a1) shows that client 1 (i.e., right triangle) and client 5 (i.e., square) extract inconsistent features (in the black box) under label skew, and Figure 2(b1) presents the feature mappings of MNIST (i.e., left and right triangles) deviate from that of SVHN (i.e., up and down triangles) under feature skew. In contrast, the feature inconsistency and classifier divergence are significantly mitigated by FedFA.

mean distance of class feature and classifier update similarity at the end of each round during training in Figure 2. Note that features are visualized according to the classes (digit dataset) owned by a client under label (feature) distribution skew and Appendix E.2 describes the specific experiment settings.

On the one hand, the existing methods (e.g., the weight-regularization-based method: FedProx and the feature-regularization-based method: MOON) still exists feature inconsistency under both label and feature distribution skews in Figure 6 and 8, such as class 1 (i.e., dark blue), class 5 (i.e., dark red) and class 9 (i.e., dark purple), but our method FedFA alleviate it significantly in Figure 2. Moreover, the existing methods have a low similarity for *positive pairs* as presented in all the histograms, indicating inconsistent feature space across clients.

On the other hand, Figure 2 reveals the simultaneous occurrence of feature inconsistency and classifier divergence (e.g., the lower the similarity of classifier updates, the more inconsistent the feature mapping between clients in Figure 2(b2) and 2(b3)). Meanwhile, as the global model converges, these two issues are only slightly alleviated under label skew, while those of feature skew even get worse. Thus, these findings show that exploring the relationship between feature and classifier updates across clients can aid in improving federated learning performance.

Theoretical demonstration. We follow (Movshovitz-Attias et al., 2017) to represent the classifier parameters ϕ_i of the i -th client as C weight vectors $\{\phi_{i,c}\}_{c=1}^C$, where $\phi_{i,c}$ is named the proxy for the c -th class samples. For simplicity, we set all the bias vectors of the classifier as zero vectors and use the cross-entropy loss as the supervised loss. The forward process of classifiers can be represented as:

$$\mathcal{L}_{\text{sup}_i}(\phi_i) := \mathbb{E}_{(\mathbf{x}_j, y_j) \in \mathcal{D}_i} [l_{\text{sup}_i}(\phi_i; (\mathbf{x}_j, y_j))] = -\frac{1}{n_i} \sum_{j=1, y_j=c}^{n_i} \log \frac{\exp(\phi_{i,c}^\top \mathbf{h}_{i,y_j})}{\sum_{q=1}^C \exp(\phi_{i,q}^\top \mathbf{h}_{i,y_j})} \quad (2)$$

where $\mathbf{h}_{i,y_j} = f_{\theta_i}(\mathbf{x}_j)$ is the feature mapping of a sample (\mathbf{x}_j, y_j) . Herein, we illustrate the relationship between classifier and feature updates across clients as follows:

Firstly, the classifier updates are diverged across clients. For the c -th local proxy $\phi_{i,c}$, the *positive features* and *negative features* denote the features from the c -th class and other classes, respectively. Let $p_{i,c}^{(j)} = \exp(\phi_{i,c}^\top \mathbf{h}_{i,y_j}) / \sum_{q=1}^C \exp(\phi_{i,q}^\top \mathbf{h}_{i,y_j})$ and we follow a mild assumption in (Wang et al., 2021b; Zhang et al., 2022) that the extracted feature $\mathbf{h}_{i,c}$ of samples and their corresponding

prediction output $p_{\cdot,c}^{(j)}$ will be similar in the same c -th class within one client (i.e., $\overline{p_{\cdot,c}^{(c)} \bar{\mathbf{h}}_{\cdot,c}} = \frac{1}{n_{\cdot,c}} \sum_{y_j=c} p_{\cdot,c}^{(j)} \mathbf{h}_{\cdot,y_j}$ where $\overline{p_{\cdot,c}^{(c)}} = \frac{1}{n_{\cdot,c}} \sum_{y_j=c} p_{\cdot,c}^{(j)}$ and $\bar{\mathbf{h}}_{\cdot,c} = \frac{1}{n_{\cdot,c}} \sum_{y_j=c} \mathbf{h}_{\cdot,y_j}$). Without losing the generality, we define classifier update deviation across clients as follows:

Definition 1 (Classifier update deviation). For client a and client b with the same sample number $n_a = n_b = n$, the deviation of classifier update $\Delta_{\phi_c}^{a,b} = \Delta\phi_{a,c} - \Delta\phi_{b,c}$ can be defined as $\Delta_{\phi_c}^{a,b} = \frac{\eta}{n} \left[\underbrace{\left(n_{a,c} \left(1 - \overline{p_{a,c}^{(c)}} \right) \bar{\mathbf{h}}_{a,c} - n_{b,c} \left(1 - \overline{p_{b,c}^{(c)}} \right) \bar{\mathbf{h}}_{b,c} \right)}_{\text{deviation by mean positive features: } \Delta_{\phi_c}^{(+),a,b}} - \underbrace{\left(\sum_{\bar{c}_a \neq c} n_{a,\bar{c}_a} \overline{p_{a,\bar{c}_a}^{(c)}} \bar{\mathbf{h}}_{a,\bar{c}_a} - \sum_{\bar{c}_b \neq c} n_{b,\bar{c}_b} \overline{p_{b,\bar{c}_b}^{(c)}} \bar{\mathbf{h}}_{b,\bar{c}_b} \right)}_{\text{deviation by mean negative features: } \Delta_{\phi_c}^{(-),a,b}} \right]$

where η is learning rate, $n_{\cdot,c}$ and class $\bar{c}_{(\cdot)}$ is sample number and one of negative classes of the c -th class (e.g., $\bar{c}_a \in \{[C_a] \setminus c\}$) of one client, respectively. The proof can be found in Appendix G.1.

For convenience of analysis, we assume that clients a and b would hold the same samples if their datasets have the same class under label distribution skew, and clients have all classes in their datasets under feature distribution skew. At the start of each round, they share the same model, and we have:

Theorem 1 (Classifier update divergence under data heterogeneity). For label distribution skew ($[C_a] \neq [C_b]$), when $c \in [C_a] \cap [C_b]$, $\bar{\mathbf{h}}_{a,c} = \bar{\mathbf{h}}_{b,c}$, $\overline{p_{a,c}^{(c)}} = \overline{p_{b,c}^{(c)}}$ and $\Delta_{\phi_c}^{(+),a,b} = 0$, and then $\|\Delta_{\phi_c}^{a,b}\|^2 = \frac{\eta^2}{n^2} \|\Delta_{\phi_c}^{(-),a,b}\|^2 > 0$; when $c \in [C] \setminus \{[C_a] \cup [C_b]\}$, $n_{a,c} = n_{b,c} = 0$ and $\Delta_{\phi_c}^{(+),a,b} = 0$, and then $\|\Delta_{\phi_c}^{a,b}\|^2 = \frac{\eta^2}{n^2} \|\Delta_{\phi_c}^{(-),a,b}\|^2 > 0$; when $c \in [C_a] \setminus \{[C_a] \cap [C_b]\}$ or $c \in [C_b] \setminus \{[C_a] \cap [C_b]\}$, $n_{a,c} = 0$ or $n_{b,c} = 0$, and then $\|\Delta_{\phi_c}^{a,b}\|^2 > 0$. For feature distribution skew, we have $\bar{\mathbf{h}}_{a,c} \neq \bar{\mathbf{h}}_{b,c}$, and then $\|\Delta_{\phi_c}^{a,b}\|^2 > 0$. The proof can be found in Appendix G.2.

Theorem 1 reveals that both label skew and feature skews diverge the classifier updates across clients, which explains the classifier divergence observed in (Luo et al., 2021).

Next, the diverged classifiers would induce feature inconsistency across clients. We define the feature deviation \mathbf{h}_{\cdot,y_j} of the same given samples across client models as follows:

Definition 2 (Feature update deviation). For client a and client b given the same n samples of one class, the update deviation of the mean class-feature $\Delta_{\mathbf{h}_c}^{a,b} = \Delta\bar{\mathbf{h}}_{a,c} - \Delta\bar{\mathbf{h}}_{b,c}$ is defined as:

$$\Delta_{\mathbf{h}_c}^{a,b} = \eta \left[\underbrace{\left((1 - \overline{p_{a,c}^{(c)}}) \phi_{a,c} - (1 - \overline{p_{b,c}^{(c)}}) \phi_{b,c} \right)}_{\text{mean deviation by positive classifier proxy: } \Delta_{\mathbf{h}_c}^{(+),a,b}} - \underbrace{\left(\sum_{\bar{c}} \overline{p_{a,\bar{c}}^{(c)}} \phi_{a,\bar{c}} - \sum_{\bar{c}} \overline{p_{b,\bar{c}}^{(c)}} \phi_{b,\bar{c}} \right)}_{\text{mean deviation by negative classifier proxy: } \Delta_{\mathbf{h}_c}^{(-),a,b}} \right]$$

where $\bar{c} \in \{[C] \setminus c\}$. The proof can be found in Appendix G.3.

According to Theorem 1, all classifier proxies under data heterogeneity have $\phi_{a,c} \neq \phi_{b,c}$, inducing $\Delta_{\mathbf{h}_c}^{(+),a,b} \neq \Delta_{\mathbf{h}_c}^{(-),a,b}$ generally. Thus, $\|\Delta_{\mathbf{h}_c}^{a,b}\|^2 > 0$, and feature updates are inconsistent across clients.

Finally, we conclude the relationship between classifier divergence and feature inconsistency as:

Theorem 2 (Relationship between classifier deviation and feature deviation) Combining Definitions 1 and 2, for client a and client b with output $\overline{p_{a,c}^{(c)}} = \overline{p_{b,c}^{(c)}}$ and $\overline{p_{a,\bar{c}}^{(c)}} = \overline{p_{b,\bar{c}}^{(c)}}$ on the c -th class and the same sample numbers $n_{a,c} = n_{b,c}$, the relationship between their classifier update divergence and feature inconsistency is $\Delta_{\mathbf{h}_c}^{a,b} = \sum_{\hat{c} \in [C]} \overline{p_{b,\hat{c}}^{(c)}} \Delta_{\phi_{\hat{c}}}^{a,b} - \eta \Delta_{\phi_c}^{a,b}$. The proof can be found in Appendix G.3.

Observation 1 (A vicious cycle) The meaning of Theorem 2 unravels that data heterogeneity firstly induces classifier updates diverged, and then diverged classifiers make inconsistent feature maps, and these inconsistent features in turn force different classifiers more diverged, as described in the toy example of Figure 1(a). Moreover, as shown in Figures 2(a2) and (a3), the vicious cycle does not disappear as the training of the global model becomes converging.

Hence, we believe that feature inconsistency and classifier divergence are coupled together to degrade the performance of federated learning, and only by addressing both problems at the same time break the *vicious cycle*.

4 FEDERATED LEARNING WITH FEATURE ANCHORS (FEDFA)

To break the *vicious cycle* in Theorem 2, we propose FedFA, whose pseudo-code is in Algorithm 1, to trains client models in a consistent feature space with the classifiers corresponding to this space.

Feature anchors loss. With a total of C classes in the whole dataset, the server initiates C feature anchor vectors $\{\mathbf{a}_c\}_{c=1}^C \in \mathcal{H} \times [C]$ indexed by $c \in [C]$ before training, which are to align the each-class feature mappings of feature extractors $f_{\theta_i}(\mathbf{x}) = \mathbf{h}_{i,\cdot}$ by the following loss:

$$\mathcal{L}_{\text{fa}_i}(\theta_i) := \mathbb{E}_{(\mathbf{x}_j, y_j) \in \mathcal{D}_i} [l_{\text{fa}}(\theta_i; \mathbf{a}_c, (\mathbf{x}_j, y_j), c = y_j)] = \frac{1}{2n_i} \sum_{j=1, c=y_j}^{n_i} \|\mathbf{h}_{i,c} - \mathbf{a}_c\|^2. \quad (3)$$

The feature anchor loss inspired by the center loss (Wen et al., 2016) measures the average distance between features and their corresponding feature anchors. Minimizing (3) can reduce the intra-class feature distance for a given client, as well as across all clients, as shown in Figures 1(b) and 5(c). Then, **each mini-batch update phase of local training** of FedFA is carried out as following:

Step1: optimizing local objective with feature anchor loss. FedFA adds the feature anchor loss to a supervised loss (e.g., the cross-entropy loss as shown in (2) represented as l_{sup}) in the local optimization. At the start of t -th round, the server sends the current global model $\mathbf{w}^{(t-1)}$ and feature anchors $\{\mathbf{a}_c^{(t-1)}\}_{c=1}^C$ to a set \mathcal{S} of active clients, and then each client $i \in \mathcal{S}$ locally updates $\mathbf{w}^{(t-1)}$ to $\mathbf{w}_i^{(t)}$ and with a mini-batch gradient descent from the following objective:

$$\min_{\mathbf{w}_i} \mathcal{L}_i(\mathbf{w}_i) := \mathcal{L}_{\text{sup}_i}(\mathbf{w}_i) + \mathcal{L}_{\text{fa}}(\theta_i) := \mathbb{E}_{(\mathbf{x}, y) \in \mathcal{D}_i} [l_{\text{sup}_i}(\mathbf{w}_i) + \mu l_{\text{fa}_i}(\theta_i)] \quad (4)$$

where $\theta_i \in \mathbf{w}_i = \{\theta_i, \phi_i\}$ and μ is a hyper parameter to balance l_{sup_i} and l_{fa_i} . The feature inconsistency caused by the divergence of feature extractors is alleviated by minimizing l_{fa_i} .

Step2: calibrating local classifier with feature anchors. Feature anchors would be used to calibrate the updates of classifier proxies after *step 1*. Specifically, at the end of each mini-batch update, the active client $i \in \mathcal{S}$ takes feature anchors $\{\mathbf{a}_c^{(t-1)}\}_{c=1}^C$ as one mini-batch input of its classifier f_{ϕ_i} and their corresponding classes as the label set $\overline{[C_i]}$ to calibrate classifiers by the objective:

$$\min_{\phi_i} \mathcal{L}_{\text{cal}_i}(\phi_i) := \mathbb{E}_{\mathbf{a}_c \in \{\mathbf{a}_c\}_{c=1}^C} [l_{\text{cal}_i}(\phi_i; (\mathbf{a}_c, c))] = -\frac{1}{C} \sum_{c \in C} \log \frac{\exp(\phi_{i,c}^\top \mathbf{a}_c)}{\sum_{q=1}^C \exp(\phi_{i,q}^\top \mathbf{a}_c)}. \quad (5)$$

The classifier calibration loss l_{cal_i} can correct the classifier divergence and keep classifiers similar at the beginning of each mini-batch update by reducing the angle between the c -th class proxy and feature anchor, thus preventing feature inconsistency as shown in Figures 1(b) and 5(c).

Step3: fixing feature anchors in local training but accumulating class features by momentums. If feature anchors $\{\mathbf{a}_c^{(t-1)}\}_{c=1}^C$ are updated locally based on gradient descent like (Wen et al., 2016), the updates of $\mathbf{a}_c^{(t-1)}$ would be inconsistent across clients under heterogeneous data. Therefore, to keep \mathbf{a}_c consistent in the k -th local epoch, client i does not update $\mathbf{a}_c^{(t-1)}$, but accumulate the c -th class features of the τ -th batch $\mathcal{B}_i^{(t,k_\tau)}$ as momentum $\mathbf{m}_{c,i}^{(t,k_\tau)} = \mathbf{m}_{c,i}^{(t,k_{\tau-1})} + \frac{1}{B|\mathcal{B}_{i,c}^{(t,k_\tau)}|} \sum_{(\mathbf{x}, c) \in \mathcal{B}_{i,c}^{(t,k_\tau)}} f_{\theta_i}(\mathbf{x})$ where B represents the total mini-batch number of one epoch and $\mathbf{m}^{(t,k_0)} = 0$. Herein, to reduce computation, we take epoch momentums $\mathbf{m}_{c,i}^{(t,k)}$ to estimate the class features by $\bar{\mathbf{a}}_{c,i}^{(t,k)} = \lambda \mathbf{m}_{c,i}^{(t,k-1)} + (1 - \lambda) \mathbf{m}_{c,i}^{(t,k)}$, instead of computing them with training dataset after local training.

Feature anchor aggregation at server. The server performs weighted averaging on all the c -th class feature $\bar{\mathbf{a}}_{c,i}^{(t,K)}$ of active clients to generate the next-round feature anchors $\{\mathbf{a}_c^{(t)}\}_{c=1}^C$, where K represents the total number of local epoch. The update of feature anchors is the same as federated model aggregation and is represented as $\mathbf{a}_c^{(t)} = \sum_{i \in \mathcal{S}} \frac{n_i}{n_s} \mathbb{E}(\mathbf{a}_{c,i}) = \sum_{i \in \mathcal{S}} \frac{n_i}{n_s} \bar{\mathbf{a}}_{c,i}^{(t,K)}$.

Theoretical analysis of FedFA. With the property of feature anchor loss (3), the feature polymerization in Figures 5 and 7 supports to assume $\bar{\mathbf{h}}_{\cdot, c} = \mathbf{a}_c$ in the following analysis.

Theorem 3 (*The effect of FedFA on the Lipschitzness of the loss on classifier weight*) *Let $\|\nabla_{\phi_c} \hat{\mathcal{L}}\|^2$ and $\|\nabla_{\phi_c} \mathcal{L}\|^2$ is the gradient norm of FedFA and FedAvg, respectively. For $\mathbf{a}_c \cdot \mathbf{a}_{\bar{c}} = 0$, the deviation of gradient norm of the global classifier between FedFA and FedAvg is computed as:*

$$\|\nabla_{\phi_c} \hat{\mathcal{L}}\|^2 - \|\nabla_{\phi_c} \mathcal{L}\|^2 = \|\Delta \hat{\phi}_c\|^2 - \|\Delta \phi_c\|^2 = \frac{\eta^2}{n^2} [(\hat{A}_c^2 - A_c^2) \|\mathbf{a}_c\|^2 + \sum_{\bar{c} \neq c} (\hat{B}_{\bar{c}}^2 - B_{\bar{c}}^2) \|\mathbf{a}_{\bar{c}}\|^2] < 0$$

where $A_c = \sum_i^N (n_{i,c}(1 - \bar{p}_{i,c}^{(c)}))$, $\hat{A}_c = \sum_i^N (n_{i,c}(1 - \hat{p}_{i,c}^{(c)}))$, $B_{\bar{c}} = \sum_i^N n_{i,\bar{c}} \bar{p}_{i,c}^{(\bar{c})}$, $\hat{B}_{\bar{c}} = \sum_i^N n_{i,\bar{c}} \hat{p}_{i,c}^{(\bar{c})}$ and $\hat{A}_c < \hat{A}_c$, $\hat{B}_{\bar{c}} < \hat{B}_{\bar{c}}$. Note that $\mathbf{a}_c \cdot \mathbf{a}_{\bar{c}} = 0$ provides an orthogonal initialization for feature anchors of FedFA. The proof can be found in Appendix G.4.

Observation 2 (*A virtuous cycle in FedFA*) *Combining Theorem 2 and Theorem 3, feature alignment and classifier calibration together smooth the loss of classifier updates to boost classifier harmony across clients, which in turn promotes feature mapping consistency across clients, as described in the toy example of Figure 1(b).*

Different from Observation 1, FedFA breaks the *vicious cycle* to obtain a *virtuous cycle* between feature and classifier updates under both label distribution skew and feature distribution skew, as shown in Figures 2(b2) and (b3). Moreover, the histograms of Figures 5(c) and 7(c) show that FedFA improves the feature polymerization for *positive pairs* and discrimination for *negative pairs* (i.e., FedFA can reduce intra-class feature distance and increase inter-class feature distance across clients to help classification).

5 EXPERIMENTS

We briefly describe our experimental setup and have more descriptions in Appendix E.

Datasets. This work aims at image classification tasks under label and feature distribution skews, and it uses federated benchmark datasets as (McMahan et al., 2017; Yurochkin et al., 2019; Li et al., 2021a), including EMNIST(Cohen et al., 2017), FMNIST(Xiao et al., 2017), CIFAR-10, CIFAR-100 (Krizhevsky et al., 2009), and Mixed Digits dataset (Li et al., 2021c). Specifically, for label distribution skew, we consider two settings: (i) Same size of local dataset: following (McMahan et al., 2017), we split data samples based on class to clients (e.g., $\#C = 2$ denotes that each client holds two class samples); (ii) Different sizes of local dataset: following (Yurochkin et al., 2019), we set α of Dirichlet distribution $Dir(\alpha)$ as 0.1 and 0.5 to generate distribution $p_{i,c}$ by which the c -th class samples are splitted to client i . For feature distribution skew, we consider two settings: (i) Real-world feature skew: we sample a subset with 10 classes of a real-world dataset EMNIST(Cohen et al., 2017) with natural feature skew; (ii) Artificial feature skew: we use a mixed-digit dataset from (Li et al., 2021c) consisting of MNIST(LeCun et al., 1998), SVHN(Netzer et al., 2011), USPS(Hull, 1994), SynthDigits and MNIST-M(Ganin et al., 2015).

Baselines and models. We compare FedFA with the canonical method FedAvg, model-weight-based methods FedProx(Li et al., 2020) and FedDyn (Acar et al., 2021), and feature-based methods MOON (Li et al., 2021b) and FedProc (Mu et al., 2021). For a fair comparison, our models follow what is reported in the baselines. Following (Acar et al., 2021), we use a CNN model with two convolution layers for EMNIST, FMNIST, and CIFAR-10. We utilize the ResNet-18 (He et al., 2016) with a linear projector from (Li et al., 2021b) for CIFAR-100 and a CNN model with three convolutional layers from (Li et al., 2021c) for Mixed Digits.

Anchor initialization and federated setup. According to Theorem 3, we initiate the pairwise-orthogonal feature anchors \mathbf{a}_c by sampling column vector from an identity matrix whose dimension is the same as features. In Tables 1 and 2, 100 clients attend federated training, 10 clients participate in each round, the local batch size is 64, the local epochs number is 5, and the targeted communication round is 200. We use the SGD optimizer with a 0.01 learning rate and 0.001 weight decay for all experiments except for the CIFAR-100 experiment with 0.9 momentum additionally. In Table 3,

Table 1: The top-1 accuracy of FedFA and all the baselines under label distribution skew on the test datasets. We run three trials and report the mean and standard derivation. For FedAvg and FedFA, we also report their top-1 accuracy without label skew.

Method (lr = 0.01)	Label Distribution Skew							
	FMNIST			CIFAR-10			CIFAR-100	
	#C = 2	$\alpha = 0.1$	$\alpha = 0.5$	#C = 2	$\alpha = 0.1$	$\alpha = 0.5$	#C = 20	$\alpha = 0.1$
FedAvg w/o skew		85.90(0.14)			59.66(0.05)			25.37(0.28)
FedFA w/o skew		89.67(0.16)			64.95(0.53)			33.94(0.44)
FedAvg	74.60(1.42)	69.81(3.00)	82.80(0.65)	36.07(3.02)	35.20(3.72)	48.66(3.00)	22.62(0.84)	21.79(0.79)
FedProx	74.63(1.30)	69.59(2.99)	82.92(0.38)	36.63(2.64)	35.21(3.78)	48.43(2.27)	22.27(0.90)	22.30(0.47)
FedDyn	74.77(1.76)	70.09(2.24)	83.95(0.29)	36.11(3.35)	36.00(3.78)	50.46(2.33)	13.28(2.19)	1.00(0.00)
MOON	74.25(1.59)	68.52(2.26)	82.72(0.42)	35.90(3.17)	34.89(3.18)	48.74(2.45)	22.03(1.00)	22.04(0.62)
FedProc	74.96(1.94)	69.80(3.26)	82.94(0.34)	36.57(3.61)	35.02(4.53)	48.99(2.85)	23.00(0.35)	22.32(0.63)
FedFA (Our)	84.08(1.22)	83.42(1.14)	88.40(0.12)	52.64(1.46)	52.95(2.01)	60.40(0.38)	26.68(1.18)	24.05(2.32)
								29.16(1.03)

Figures 3 and 4, we follow the setup (Li et al., 2021b) to investigate the impact of different federated setup with 200 rounds and a local SGD with a 0.01 learning rate and 0.9 momentum on CIFAR-10.

Performance under label distribution skew. Table 1 shows that FedFA provides significant gains in different label-skew settings regardless of the dataset. Compared with $\alpha = 0.5$, both $\#C = 2$ and $\alpha = 0.1$ indicate more severe label distribution skew, but clients under $\#C = 2$ have the same sample number while the ones with $\alpha = 0.1$ do not. Firstly, we find that the performance of all methods decreases as the degree of data heterogeneity increases. Nevertheless, the decline of FedFA is much smaller than that of other methods. For example, when α changes from 0.5 to 0.1, the top-1 accuracy of all the baselines goes down by about 13% on FMNIST and CIFAR-10, which is twice as large as FedFA. Secondly, under the same label skew, FedFA achieves larger gains over other methods when label distribution skew becomes more severe, up to 18.06% (i.e., Moon: 34.89% and FedFA 52.95% under $\alpha = 0.1$ in CIFAR-10). Thirdly, to explore more difficult tasks, we test on CIFAR-100 with ResNet18, and our method still achieves the best performance (i.e., about 3% accuracy advance).

Performance under feature distribution skew. According to Table 2, our method obtains higher accuracy than all baselines on EMNIST and Mixed Digits. Specifically, the accuracy of FedFA in EMNIST reaches 99.28%, which is 0.77% higher than the best baseline (i.e., MOON 98.51%). Moreover, we split each digit dataset of Mixed Digits into 20 subsets, one for each client with the same sample number (e.g., a skewed feature distribution exists between the clients

Table 2: The top-1 accuracy of all methods under label & feature distribution skews on the test dataset. Note that we report the average top-1 accuracy on five benchmark digit datasets in Mixed Digit.

Method	Feature Distribution Skew		Label & Feature Distribution Skew		
	EMNIST	Mixed Digits	#C = 2	Mixed Digits $\alpha = 0.1$	$\alpha = 0.5$
FedAvg w/o skew	-			82.66(2.38)	
FedFA w/o skew	-			88.10(0.39)	
FedAvg	98.50(0.04)	82.66(2.83)	56.13(5.59)	63.74(2.35)	78.34(1.58)
FedProx	98.44(0.06)	82.46(2.65)	54.86(5.80)	62.57(2.22)	78.08(1.84)
FedDyn	97.63(0.19)	83.59(2.33)	51.66(7.33)	63.55(2.02)	79.40(1.76)
MOON	98.51(0.06)	81.46(2.84)	55.40(5.69)	62.18(1.93)	78.05(1.82)
FedProc	98.28(0.04)	82.06(2.68)	59.53(3.66)	64.59(2.15)	78.66(1.16)
FedFA	99.28(0.33)	90.73(2.01)	83.46(2.57)	85.71(0.71)	89.82(0.49)

with a subset of SVHN and the ones with a subset of MNIST). Compared with the best baseline (i.e., Feddyn: 83.59%) on Mixed Digits, our method achieves performance gains of 7.14%.

Performance under combined label and feature distribution skews. We combine label skew and feature skew to explore the impact of data heterogeneity further. Namely, we not only split each dataset in Mixed Digits into 20 subsets, one for each client, but also set the different label distributions for each client (i.e., clients are subject to at least one of label distribution skew and feature distribution skew). The results in Table 2 show that all the methods are more susceptible under this setting than that of feature distribution skew. For example, the most significant performance drop reaches 31.93% (i.e., FedDyn from 83.59% to 51.66% under $\#C = 2$). Nevertheless, FedFA significantly mitigates this performance degradation with a mild decrease from 90.73% to 83.46%. Meanwhile, FedFA keep at least 10% performance advantage than all baselines under this case, where the largest gap can reach 31.8% (i.e., FedFA from 83.59% to FedDyn 51.66% under $\#C = 2$).

Performance without label or feature distribution skew. We compare our method with FedAvg under more homogeneous data and take the same learning rate of this case as that of data heterogeneity for comparison, where the results are reported in Table 1 and Table 2. The results demonstrate that FedFA still brings a significant advance in the presence of data homogeneity. For example, FedFA is 8.64% more accurate than FedAvg on CIFAR-100. Incredibly, FedFA under mild data heterogeneity (e.g., $\alpha = 0.5$ in FMNIST or Mixed Digits) even obtains higher accuracy than FedAvg without any

label or feature skew (e.g., FedFA: 88.40% vs. FedAvg: 85.90% in FMNIST). This illustrates the importance of guaranteeing the consistency of feature mappings.

Performance under local SGD with momentum. (Yu et al., 2019) found that the local optimizer with momentum is more robust to different Lipschitzness of loss to improve generalization more well. We explore the effect of FedFA on the loss Lipschitzness by comparing local SGD optimizers with momentum and without momentum on CIFAR-10. Note that FedDyD and FedProc are not compatible with the local SGD with momentum as shown in Figure 11, and thus Table 3 and Figure 3 would not include their results. Comparing Table 1 with Table 3, all methods with momentum work better than that without momentum, but FedFA without momentum has superior performance than baselines with momentum under $\#C = 2$ and $\alpha = 0.1$ (e.g., FedFA without momentum: 52.95% vs. FedProx with momentum: 49.87% under $\alpha = 0.1$), which indicates the smoother loss of FedFA than baselines, as analyzed in Theorem 3.

Performance under different client sample rate and local epoch. As shown in Figure 3(a), larger client sample rate achieves better test accuracy for all methods, especially, the about 10% accuracy gains from sample rate 0.1 to 0.3 is much larger than that from 0.3 to 0.5. As shown in Figure 3(b), larger local epochs have a negative impact on performance but FedProx and MOON have worse performance degradation than FedAvg and FedFA. Besides, the performance advantage of FedFA under different batch size is shown in Figures 12 and 13. Overall, our method FedFA consistently performs better performance than all baselines under different federated setups.

Ablation study on FedFA. As shown in Table 4, we conduct ablation studies on FedFA without anchor updating in (4), FedFA without classifier calibration in (5), and FedFA without orthogonal anchor initialization according to Property 4 to give an intuition of FedFA performance. More ablation research have been conducted on the effects of anchor initialization and anchor momentum updates on FedFA as well as the ideal times to calibrate classifiers in Appendix B.2.1 and B.2.2. First, under both label and feature distribution skews, the anchor updating brings consistent performance benefits (i.e., at least around 2% boost) to FedFA since the updated anchors can keep client models more expressive in the shared feature space. Second, classifier calibration plays the most crucial role in FedFA under both label and feature skew because the skew induces a low classifier update similarity observed in Figure 2. Third, as shown in Figure 10, orthogonal initialization provides a good initialization point for feature anchors though it does not provide a large performance gains at the final performance under both label and feature skew. Overall, FedFA promotes a shared feature space among clients and keeps classifiers consistent in this space to overcome data heterogeneity.

Ablation study on FedFA with different μ on convergence. We perform an experiment to explore the effect of different μ in (4) on the convergence rate of FedFA, whose setting is the same as Figure 3 based on CIFAR-10 with $\alpha = 0.5$, as shown in Figure 4. According to the results, when $\mu > 4$, the model converges quite slow, and $\mu < 1$ yield a similar convergence rate. In our experiments, $\mu = 0.1$ achieves the best performance.

Due to the page limitation, Appendix B presents more experiment results, e.g., feature visualization, different client numbers, when to calibrate classifiers and different initialization methods for feature anchors.

Table 3: Accuracy under local SGD with momentum.

Method (lr 0.01 w/ 0.9M)	#C = 2	CIFAR-10	
		$\alpha = 0.1$	$\alpha = 0.5$
FedAvg w/o skew		67.58(0.23)	
FedFA w/o skew		69.32(0.36)	
FedAvg	48.17(3.40)	47.91(5.95)	64.12(1.02)
FedProx	48.14(2.89)	49.87(6.82)	63.71(1.15)
MOON	48.13(2.12)	47.11(6.96)	64.08(1.20)
FedFA (Our)	57.30(2.05)	54.21(5.55)	64.63(0.57)

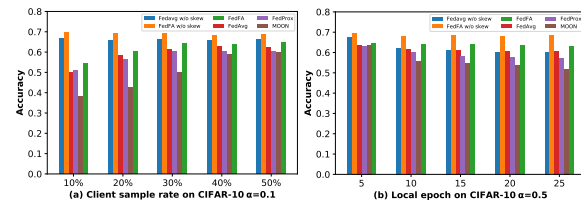


Figure 3: Accuracy under different federated setting.

Table 4: The top-1 accuracy of FedFA in different ablation.

Method (lr = 0.01)	Label Skew (FMNIST $\#C = 2$)	Feature Skew (Mixed Digits)	Label & Feature Skew (Mixed Digits $\#C = 2$)
FedFA w/o anchor updating	81.89(1.87)	88.69(0.75)	76.81(1.78)
FedFA w/o classifier calibration	78.07(2.23)	79.25(1.25)	61.36(4.00)
FedFA w/o orthogonal anchor initialization	83.96(1.27)	90.76(0.54)	83.34(1.42)
FedFA (Our)	84.08(1.22)	90.86(1.92)	83.73(2.76)

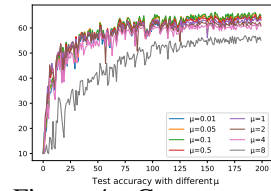


Figure 4: Convergence with different μ .

6 CONCLUSION

This work focuses on alleviating performance degradation caused by label and feature distribution skews in federated learning. Firstly, we observe and analyze the existence of a *vicious cycle* between feature mapping inconsistency and classifier update divergence under data heterogeneity. Secondly, we propose FedFA to create a shared feature space across clients, assisted by feature anchors, and keep the classifier consistent in this space, thus bringing a *virtuous cycle* between feature and classifier updates. Finally, FedFA significantly outperforms baselines on various image classification tasks.

REFERENCES

Durmus Alp Emre Acar, Yue Zhao, Ramon Matas, Matthew Mattina, Paul Whatmough, and Venkatesh Saligrama. Federated learning based on dynamic regularization. In *International Conference on Learning Representations*, 2021. URL <https://openreview.net/forum?id=B7v4QMR6Z9w>.

Maruan Al-Shedivat, Jennifer Gillenwater, Eric Xing, and Afshin Rostamizadeh. Federated learning via posterior averaging: A new perspective and practical algorithms. In *International Conference on Learning Representations*, 2021. URL <https://openreview.net/forum?id=GfSu8a0sGB>.

Hong-You Chen and Wei-Lun Chao. On bridging generic and personalized federated learning for image classification. In *International Conference on Learning Representations*, 2022. URL <https://openreview.net/forum?id=I1hQbx10Kxn>.

Gregory Cohen, Saeed Afshar, Jonathan Tapson, and Andre Van Schaik. Emnist: Extending mnist to handwritten letters. In *2017 international joint conference on neural networks*, pp. 2921–2926. IEEE, 2017.

Alireza Fallah, Aryan Mokhtari, and Asuman Ozdaglar. Personalized federated learning: A meta-learning approach. *arXiv preprint arXiv:2002.07948*, 2020.

Ganin, Yaroslav, Lempitsky, and Victor. Unsupervised domain adaptation by backpropagation. In *International Conference on Machine Learning*, pp. 1180–1189. PMLR, 2015.

Chaoyang He, Alay Dilipbhai Shah, Zhenheng Tang, Di Fan1Adarshan Naiynar Sivashunmugam, Keerti Bhogaraju, Mita Shimpi, Li Shen, Xiaowen Chu, Mahdi Soltanolkotabi, and Salman Avestimehr. Fedcv: a federated learning framework for diverse computer vision tasks. *arXiv preprint arXiv:2111.11066*, 2021.

Kaiming He, Xiangyu Zhang, Shaoqing Ren, and Jian Sun. Deep residual learning for image recognition. In *Proceedings of the IEEE conference on computer vision and pattern recognition*, pp. 770–778, 2016.

Kevin Hsieh, Amar Phanishayee, Onur Mutlu, and Phillip Gibbons. The non-iid data quagmire of decentralized machine learning. In *International Conference on Machine Learning*, pp. 4387–4398. PMLR, 2020.

Jonathan J. Hull. A database for handwritten text recognition research. *IEEE Transactions on pattern analysis and machine intelligence*, 16(5):550–554, 1994.

Peter Kairouz, H Brendan McMahan, Brendan Avent, Aurélien Bellet, Mehdi Bennis, Arjun Nitin Bhagoji, Kallista Bonawitz, Zachary Charles, Graham Cormode, Rachel Cummings, et al. Advances and open problems in federated learning. *Foundations and Trends® in Machine Learning*, 14(1–2):1–210, 2021.

Sai Praneeth Karimireddy, Satyen Kale, Mehryar Mohri, Sashank Reddi, Sebastian Stich, and Ananda Theertha Suresh. Scaffold: Stochastic controlled averaging for federated learning. In *International Conference on Machine Learning*, pp. 5132–5143. PMLR, 2020.

Alex Krizhevsky, Geoffrey Hinton, et al. Learning multiple layers of features from tiny images. 2009.

Yann LeCun, Léon Bottou, Yoshua Bengio, and Patrick Haffner. Gradient-based learning applied to document recognition. *Proceedings of the IEEE*, 86(11):2278–2324, 1998.

Qinbin Li, Yiqun Diao, Quan Chen, and Bingsheng He. Federated learning on non-iid data silos: An experimental study. *arXiv preprint arXiv:2102.02079*, 2021a.

Qinbin Li, Bingsheng He, and Dawn Song. Model-contrastive federated learning. In *Proceedings of the IEEE/CVF Conference on Computer Vision and Pattern Recognition*, pp. 10713–10722, 2021b.

Tian Li, Anit Kumar Sahu, Manzil Zaheer, Maziar Sanjabi, Ameet Talwalkar, and Virginia Smith. Federated optimization in heterogeneous networks. *Proceedings of Machine Learning and Systems*, 2:429–450, 2020.

Xiaoxiao Li, Meirui Jiang, Xiaofei Zhang, Michael Kamp, and Qi Dou. Fedbn: Federated learning on non-iid features via local batch normalization. In *International Conference on Learning Representations*, 2021c. URL <https://openreview.net/pdf?id=6YEQUn0QICG>.

Xin-Chun Li and De-Chuan Zhan. Fedrs: Federated learning with restricted softmax for label distribution non-iid data. In *Proceedings of the 27th ACM SIGKDD Conference on Knowledge Discovery & Data Mining*, pp. 995–1005, 2021.

Zijian Li, Jiawei Shao, Yuyi Mao, Jessie Hui Wang, and Jun Zhang. Federated learning with gan-based data synthesis for non-iid clients. *arXiv preprint arXiv:2206.05507*, 2022.

Mi Luo, Fei Chen, Dapeng Hu, Yifan Zhang, Jian Liang, and Jiashi Feng. No fear of heterogeneity: Classifier calibration for federated learning with non-iid data. *Advances in Neural Information Processing Systems*, 34:5972–5984, 2021.

Brendan McMahan, Eider Moore, Daniel Ramage, Seth Hampson, and Blaise Aguera y Arcas. Communication-efficient learning of deep networks from decentralized data. In *Artificial intelligence and statistics*, pp. 1273–1282. PMLR, 2017.

Yair Movshovitz-Attias, Alexander Toshev, Thomas K Leung, Sergey Ioffe, and Saurabh Singh. No fuss distance metric learning using proxies. In *Proceedings of the IEEE International Conference on Computer Vision*, pp. 360–368, 2017.

Xutong Mu, Yulong Shen, Ke Cheng, Xueli Geng, Jiaxuan Fu, Tao Zhang, and Zhiwei Zhang. Fedproc: Prototypical contrastive federated learning on non-iid data. *arXiv preprint arXiv:2109.12273*, 2021.

Yuval Netzer, Tao Wang, Adam Coates, Alessandro Bissacco, Bo Wu, and Andrew Y Ng. Reading digits in natural images with unsupervised feature learning. 2011.

Adam Paszke, Sam Gross, Francisco Massa, Adam Lerer, James Bradbury, Gregory Chanan, Trevor Killeen, Zeming Lin, Natalia Gimelshein, Luca Antiga, et al. Pytorch: An imperative style, high-performance deep learning library. *Advances in Neural Information Processing Systems*, 32, 2019.

Sashank J. Reddi, Zachary Charles, Manzil Zaheer, Zachary Garrett, Keith Rush, Jakub Konečný, Sanjiv Kumar, and Hugh Brendan McMahan. Adaptive federated optimization. In *International Conference on Learning Representations*, 2021. URL <https://openreview.net/forum?id=LkFG31B13U5>.

Jiawei Shao, Yuchang Sun, Songze Li, and Jun Zhang. Dres-fl: Dropout-resilient secure federated learning for non-iid clients via secret data sharing. *Advances in Neural Information Processing Systems*, 2022.

Jake Snell, Kevin Swersky, and Richard Zemel. Prototypical networks for few-shot learning. *Advances in Neural Information Processing Systems*, 30, 2017.

Yuchang Sun, Jiawei Shao, Songze Li, Yuyi Mao, and Jun Zhang. Stochastic coded federated learning with convergence and privacy guarantees. *arXiv preprint arXiv:2201.10092*, 2022.

Canh T Dinh, Nguyen Tran, and Josh Nguyen. Personalized federated learning with moreau envelopes. *Advances in Neural Information Processing Systems*, 33:21394–21405, 2020.

Alysa Ziying Tan, Han Yu, Lizhen Cui, and Qiang Yang. Towards personalized federated learning. *IEEE Transactions on Neural Networks and Learning Systems*, 2022a.

Yue Tan, Guodong Long, Lu Liu, Tianyi Zhou, Qinghua Lu, Jing Jiang, and Chengqi Zhang. Fedproto: Federated prototype learning across heterogeneous clients. In *AAAI Conference on Artificial Intelligence*, volume 1, pp. 3, 2022b.

Zhenheng Tang, Yonggang Zhang, Shaohuai Shi, Xin He, Bo Han, and Xiaowen Chu. Virtual homogeneity learning: Defending against data heterogeneity in federated learning. In *International Conference on Machine Learning*, pp. 21111–21132, 2022.

Laurens Van der Maaten and Geoffrey Hinton. Visualizing data using t-sne. *Journal of machine learning research*, 9(11), 2008.

Hongyi Wang, Mikhail Yurochkin, Yuekai Sun, Dimitris Papailiopoulos, and Yasaman Khazaeni. Federated learning with matched averaging. In *International Conference on Learning Representations*, 2020a. URL <https://openreview.net/forum?id=BkluqlSFDS>.

Jianyu Wang, Qinghua Liu, Hao Liang, Gauri Joshi, and H Vincent Poor. Tackling the objective inconsistency problem in heterogeneous federated optimization. *Advances in Neural Information Processing Systems*, 33:7611–7623, 2020b.

Jianyu Wang, Zachary Charles, Zheng Xu, Gauri Joshi, H Brendan McMahan, Maruan Al-Shedivat, Galen Andrew, Salman Avestimehr, Katharine Daly, Deepesh Data, et al. A field guide to federated optimization. *arXiv preprint arXiv:2107.06917*, 2021a.

Lixu Wang, Shichao Xu, Xiao Wang, and Qi Zhu. Addressing class imbalance in federated learning. In *Proceedings of the AAAI Conference on Artificial Intelligence*, volume 35, pp. 10165–10173, 2021b.

Yandong Wen, Kaipeng Zhang, Zhifeng Li, and Yu Qiao. A discriminative feature learning approach for deep face recognition. In *European conference on computer vision*, pp. 499–515. Springer, 2016.

Han Xiao, Kashif Rasul, and Roland Vollgraf. Fashion-mnist: a novel image dataset for benchmarking machine learning algorithms. *arXiv preprint arXiv:1708.07747*, 2017.

Fuxun Yu, Weishan Zhang, Zhuwei Qin, Zirui Xu, Di Wang, Chenchen Liu, Zhi Tian, and Xiang Chen. Fed2: Feature-aligned federated learning. In *Proceedings of the 27th ACM SIGKDD Conference on Knowledge Discovery & Data Mining*, pp. 2066–2074, 2021.

Hao Yu, Rong Jin, and Sen Yang. On the linear speedup analysis of communication efficient momentum sgd for distributed non-convex optimization. In *International Conference on Machine Learning*, pp. 7184–7193. PMLR, 2019.

Mikhail Yurochkin, Mayank Agarwal, Soumya Ghosh, Kristjan Greenewald, Nghia Hoang, and Yasaman Khazaeni. Bayesian nonparametric federated learning of neural networks. In *International Conference on Machine Learning*, pp. 7252–7261. PMLR, 2019.

Dun Zeng, Siqi Liang, Xiangjing Hu, and Zenglin Xu. Fedlab: A flexible federated learning framework. *arXiv preprint arXiv:2107.11621*, 2021.

Jie Zhang, Zhiqi Li, Bo Li, Jianghe Xu, Shuang Wu, Shouhong Ding, and Chao Wu. Federated learning with label distribution skew via logits calibration. In *International Conference on Machine Learning*, pp. 26311–26329. PMLR, 2022.

Lin Zhang, Yong Luo, Yan Bai, Bo Du, and Ling-Yu Duan. Federated learning for non-iid data via unified feature learning and optimization objective alignment. In *Proceedings of the IEEE/CVF International Conference on Computer Vision*, pp. 4420–4428, 2021.

Yue Zhao, Meng Li, Liangzhen Lai, Naveen Suda, Damon Civin, and Vikas Chandra. Federated learning with non-iid data. *arXiv preprint arXiv:1806.00582*, 2018.

APPENDIX

A TERMINOLOGIES

Global model vs. local model. Let us first clarify the concepts of “global” vs. “local” models: in each communication round, local models denote the ones updated by the clients after local training, and the global model denotes the model obtained by aggregating all local models at the server. Moreover, client models denote the models being trained during local training.

Vicious cycle vs. virtuous cycle. As shown in Figure 1 (a), the *vicious cycle* represents the phenomenon that inconsistent feature mappings of local models diverge the classifier updates, such that the diverged classifiers of different clients induce feature extractors to map to more inconsistent features across clients. As shown in Figure 1 (b), the *virtuous cycle* represents the phenomenon that consistent feature mappings of client local models make the classifier updates similar, such that the updated classifiers make feature extractors of clients map to more consistent features across clients.

Positive pair vs. negative pair. A *positive pair* denotes a pair of **samples** with the same label (i.e., the samples belong to the same class). A *negative pair* denotes a pair of **samples** with different labels (i.e., the samples do not belong to the same class).

Positive feature vs. negative feature. For the c -th proxy ϕ_c , the *positive features* denote the **features** of the c -th class, and the *negative features* denote the **features** of other classes except for the c -th class.

Positive proxy vs. negative proxy. For the feature of the c -th class, the *positive proxy* denotes the c -th **proxy** ϕ_c , and the *negative proxies* denote other **proxies** except for the c -th proxy ϕ_c .

Label distribution skew vs. feature distribution skew. Feature and label distribution skews are two representative data heterogeneity (Kairouz et al., 2021), both covered in this work. Suppose that the i -th client data distribution follows $P_i(x, y) = P_i(x|y)P_i(y) = P_i(y|x)P_i(x)$ where x and y denote the feature and label respectively. Following (Li et al., 2021a), the definition of feature distribution skew and label distribution skew can be given as:

- **Label distribution skew (prior probability):** The label marginal distribution $P_i(y)$ varies across clients while $P_i(x|y) = P_j(x|y)$ for all clients i and j .
- **Feature distribution skew (covariate shift):** The input feature marginal distribution $P_i(x)$ varies across clients while $P_i(y|x) = P_j(y|x)$ for all clients i and j .
- **Label & feature distribution skew:** At least one of the label distribution skew and feature distribution skew happens across clients. This means clients i and j still suffer from label marginal distribution skew $P_i(y)$ even if sharing the same $P_i(x)$, or clients i and j still suffer from input feature marginal distribution skew $P_i(x)$ even if sharing the same $P_i(y)$.
- **Local data distributions without skew:** Herein, for FMNIST, CIFAR-10, and CIFAR-100, we split them evenly into client-side local datasets based on an identical label distribution. For Mixed Digits, we first mix all the digit datasets as a global dataset and evenly split it into client-side local datasets based on an identical label distribution. Note that this case can not guarantee that local distributions share the same global distribution across clients. Still, it means local distributions are more homogeneous than the cases of label or feature distribution skew.

B ADDITIONAL EXPERIMENT RESULTS

B.1 ADDITIONAL VALIDATION EXPERIMENT RESULTS

B.1.1 FEATURE VISUALIZATION AND SIMILARITY HISTOGRAM FOR ALL METHODS UNDER LABEL DISTRIBUTION SKEW

Figures 5 and 6 show the t-SNE visualization and the histogram of cosine similarity of feature mappings for label distribution skew for all methods. We observe that all baselines under label skew exist feature mapping inconsistency across clients. Still, our method FedFA alleviates it significantly,

such as class 1 (i.e., dark blue), class 5 (i.e., dark red) and class 9 (i.e., dark purple) in Figures 5 and 6. Besides, similar to the analysis of Figure 2, the histograms also show that label distribution skew could induce the lower similarity for *positive pairs*, which means feature inconsistency. Moreover, there exists a low frequency of *positive pairs* and a small gap between *positive pairs* and *negative pairs*, which indicates inconsistent polymerization and discrimination (i.e., sizeable intra-class feature distance and small inter-class feature distance) across clients in classification tasks. These results of label distribution skew reveal that all client models are trained in inconsistent feature spaces by our baselines, which hurts their performance.

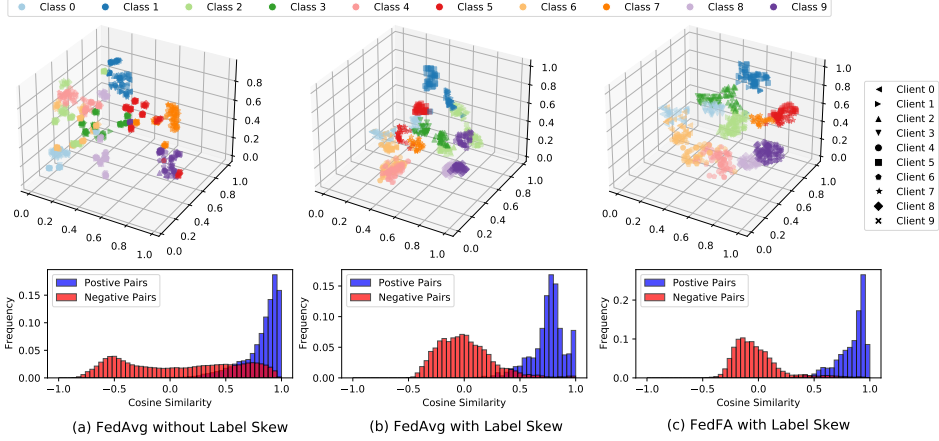


Figure 5: The t-SNE visualization and the histogram of cosine similarity of feature mappings for FedAvg under data homogeneity and for FedAvg and FedFA under label distribution skew with 10 clients.

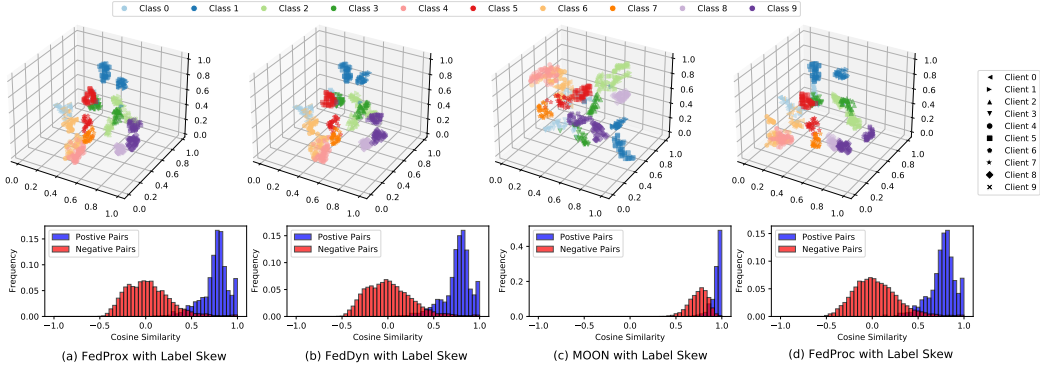


Figure 6: The t-SNE visualization and the histogram of cosine similarity of feature mappings for all baselines under label distribution skew with 10 clients.

B.1.2 FEATURE VISUALIZATION AND SIMILARITY HISTOGRAM FOR ALL METHODS UNDER FEATURE DISTRIBUTION SKEW

Similar to label distribution skew, Figures 7 and 8 show the t-SNE visualization and the histogram of cosine similarity of feature mappings for feature distribution skew for all methods. We also observe that all baselines under feature skew still suffer from feature mapping inconsistency across clients, but our method does not. Moreover, without the feature alignment, all baselines present the weak feature polymerization and feature discrimination of clients’ local models, which would make the classifier updates divergent as denoted in (1). Therefore, these results of feature distribution skew

reveal that all client models are trained in inconsistent feature spaces by our baselines, which hurts their performance.

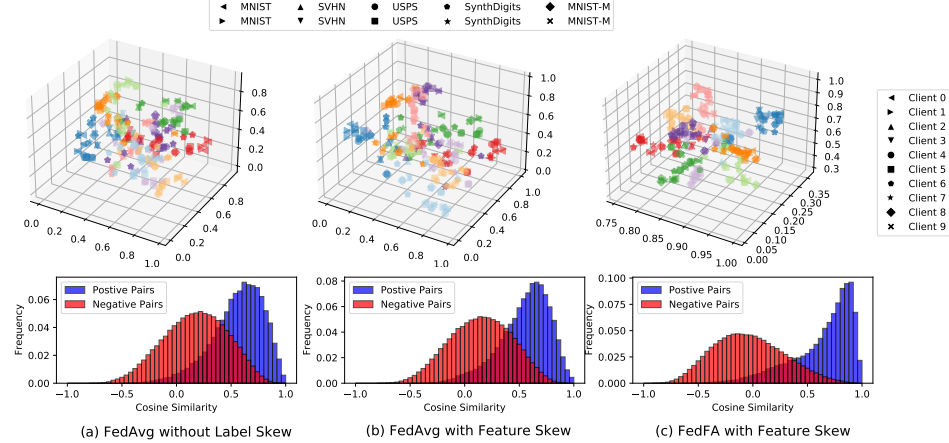


Figure 7: The t-SNE visualization and the histogram of cosine similarity of feature mappings for FedAvg under data homogeneity and for FedAvg and FedFA under feature distribution skew with 10 clients.

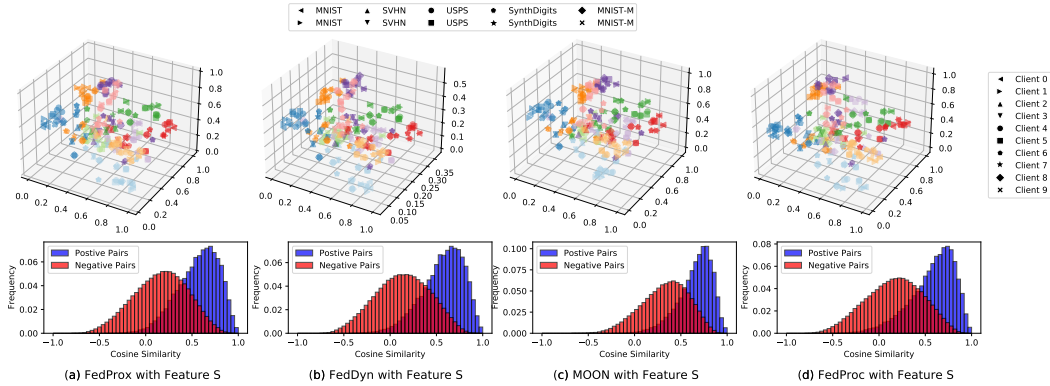


Figure 8: The t-SNE visualization and the histogram of cosine similarity of feature mappings for all baselines under feature distribution skew with 10 clients.

B.2 ADDITIONAL ABLATION EXPERIMENT RESULTS

B.2.1 ADDITIONAL ABLATION EXPERIMENTS ON CLASSIFIER CALIBRATION

Difference between classifier calibration with feature anchors and classifier calibration with virtual representations. The major difference between classifier calibration with feature anchors and classifier calibration with virtual representations (CCVR) (Luo et al., 2021) is when to calibrate classifiers in federated learning. FedFA calibrates classifiers during training (i.e., each mini-batch update phase of local training) by clients, and CCVR does it after training by the server. The goal of our local classifier calibration is to keep clients’ classifiers similar across clients at the beginning of the next mini-batch update without additional communication. We observed that this modification could bring similar classifier updates and feature consistency for federated learning, as shown in Figure 2.

When to calibrate classifier is the best? To further investigate this question, we perform the following study on the FMNIST $\#C = 2$ case whose setting is the same as Table 1, where the

Table 5: Classifier calibration at different training phase.

	Accuracy
FedAvg	73.19
FedAvg w/ CCVR	75.95
FedFA	84.90
FedFA w/o CC	76.81
FedFA w/o CC but w/ CCVR	76.94
FedFA w/ CC and CCVR	84.94
FedFA w/ CC at the end of each local epoch	82.05

term “CC” denotes local classifier calibration: The above results reveal that the best time to calibrate classifiers is during each mini-batch in local training. Meanwhile, post-calibration only improves little for FedFA, which means that keeping the virtuous cycle between feature consistency and classifier update similarity during training, as shown in Figure 1, can promote the final performance significantly.

B.2.2 ADDITIONAL ABLATION EXPERIMENTS ON FEATURE ANCHORS

The momentum update of feature anchors. We set different momentum coefficient (λ) of feature anchor updates to perform experiments on the FMNIST with $\#C = 2$ case whose setting is the same as Table 1. The results are shown as follows:

Table 6: The momentum update of feature anchors with differen λ .

λ	0	0.1	0.2	0.3	0.4	0.5	0.6	0.7	0.8	0.9	1
Accuracy	84.12	83.83	83.94	84.19	83.79	84.08	84.05	84.19	84.08	84.37	81.55

The results denote that FedFA is not sensitive to the momentum coefficient λ . When $\lambda=1$, feature anchors will not be updated, as showed in Figure 9(b). When $\lambda=0$, feature anchors will be set as the new mean feature of the last epoch. FedFA with $\lambda=0$ appears to work about as well as other cases, but it introduces more oscillations during training, as showed in Figure 9(a).

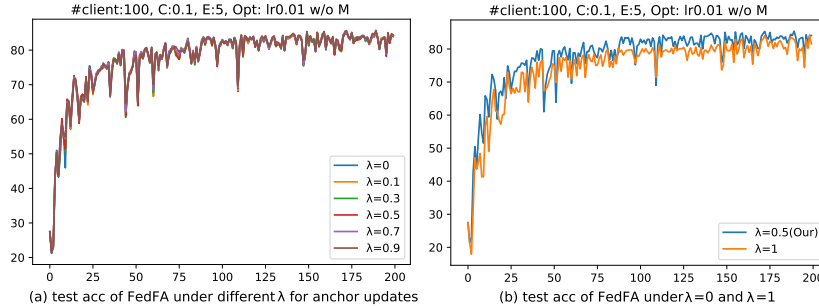


Figure 9: The updates of feature anchors of FedFA With different λ .

The initialization of feature anchors. To explore the impact of initialization of feature anchors on convergence speed, we design three experiments, including random initialization, one-round-FedAvg initialization that you suggested and “ideal” initialization. The “ideal” initialization denotes feature anchors are initiated by the trained feature anchors obtained from finishing FedFA training. The results are shown as follows:

The results reveal that the initialization of the feature anchors may not affect the convergence speed of FedFA, possibly because the anchors are updated in each communication round so that the impact of initialization of feature anchors is quickly and drastically mitigated. For example, as shown in Figure 10, FedFA with orthogonal initialization provides better accuracy than others in the first round but does not obtain the best accuracy in the final round.

Table 7: The Top-1 accuracy at the targeted round under FedFA with different initialization.

	Accuracy
FedFA (lambda=0.9)	84.37
FedFA w/ random initialization	84.07
FedFA w/ 1round FedAvg	84.94
FedFA w/ “ideal” initialization	84.33

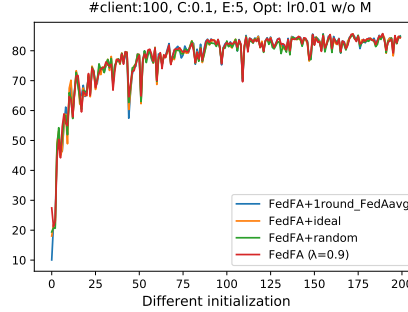


Figure 10: The feature anchors of FedFA with different initialization.

B.3 ADDITIONAL TEST EXPERIMENT RESULTS

B.3.1 PERFORMANCE UNDER LOCAL SGD WITH MOMENTUM

Given 100 clients with sample rate 0.1, we test the performance of all method with local optimizers with momentum, and report the top-1 accuracy across rounds in Figure 11. We can see that FedDyn and FedProc do not work well with local optimizers with momentum in this federated setting.

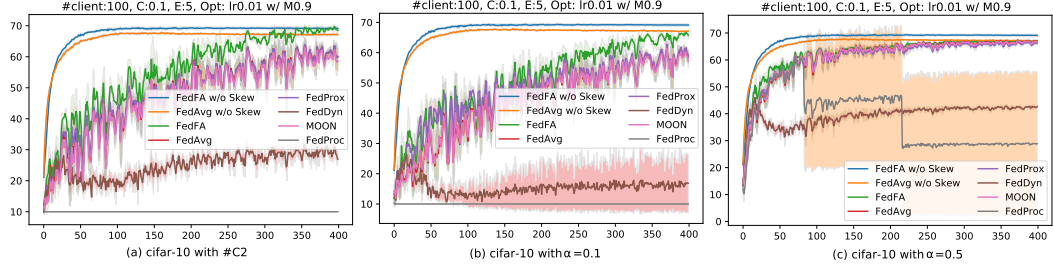


Figure 11: Performance under local SGD with momentum

B.3.2 PERFORMANCE UNDER DIFFERENT CLIENT SAMPLE RATE WITH 400 ROUNDS

Here, to ablate the impact of limited communication rounds, we report the results with 400 communication rounds in Figure 12 (a). Similar to the results of 200 rounds in Figure 3, FedFA still present about 4% accuracy advantage than other baselines.

B.3.3 PERFORMANCE UNDER DIFFERENT BATCH SIZE

Following the setup form (Li et al., 2021b), given 100 clients and 400 communication rounds, we investigate the impact of different federated setting on FedFA and baselines with SGD optimizer with a 0.01 learning rate and momentum 0.9 on CIFAR-10, including different local epoch, batch size and client sample rate , where the results are shown in Figures 3 and 12. For different local epochs, we observe that the bigger local epochs result in lower performance in all methods, FedProx and MOON

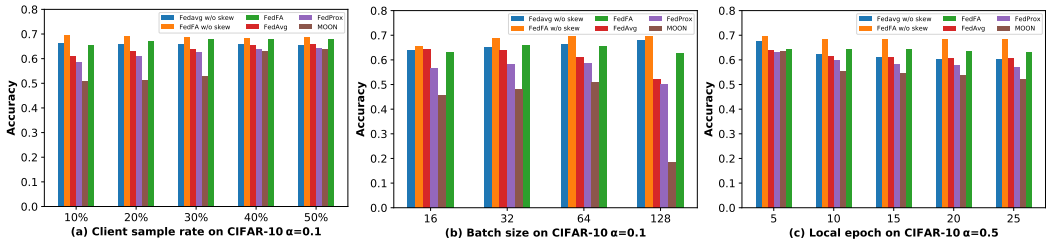


Figure 12: Performance under different (a) client sample rate, (b) batch size and (c) local epoch on CIFAR-10.

suffer from worse performance degradation than FedAvg and FedFA. For different batch sizes, 12 presents FedAvg with a relatively small batch size can work better than that of larger batch sizes, and FedFA, FedProx and MOON performs best with batch size 64. For different client sample rates, FedFA have a significant performance advantage than other methods, which demonstrates the unique advantage of FedFA in addressing data heterogeneity (i.e., it is robust to different heterogeneous Settings).

B.3.4 PERFORMANCE UNDER DIFFERENT CLIENT NUMBERS

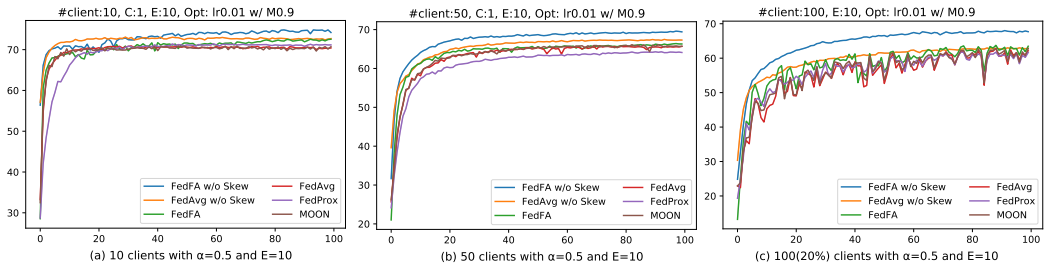


Figure 13: Performance under Different client numbers

To explore the influence of client numbers (i.e., the flexibility of FedFA for cross-silo federated learning and cross-device federated learning), we follow the setting (Li et al., 2021b) to test the performance of all method with 10 clients, 50 clients and 100 clients with 0.2 sample rate, and report the top-1 accuracy across rounds in Figure 13. We can see that FedFA keep better performance than baselines in federated learning with different client numbers.

B.3.5 TRAINING ACCURACY UNDER LABEL DISTRIBUTION SKEW

The training accuracy under label skew is shown as Figure 14 to Figure 16, which illustrates that the performance of FedFA is better than all baselines on FMNIST, CIFAR-10, and CIFAR-100. FedFA achieves better generalization than baselines on CIFAR-100 with ResNet but takes more communication rounds to converge. This observation is reasonable because regularizing only the penultimate layer by feature anchor loss takes more time to align the feature maps of the shallow layers, which we will explore in future work.

B.3.6 TRAINING ACCURACY UNDER FEATURE DISTRIBUTION SKEW

Figures 17 to 18 show the better performance of FedFA over all baselines under feature distribution skew on EMNIST and Mixed Digit.

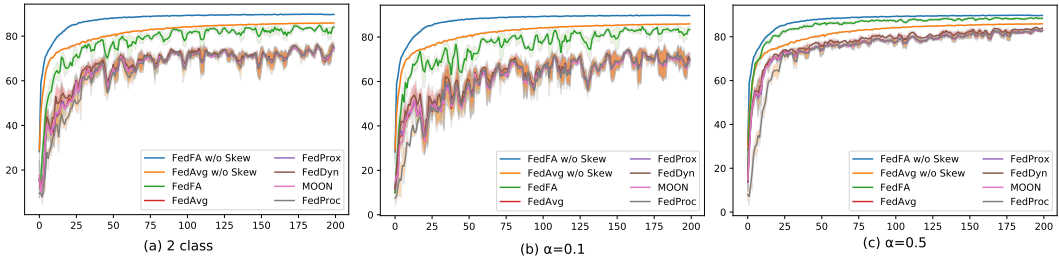


Figure 14: FMNIST with label skew.

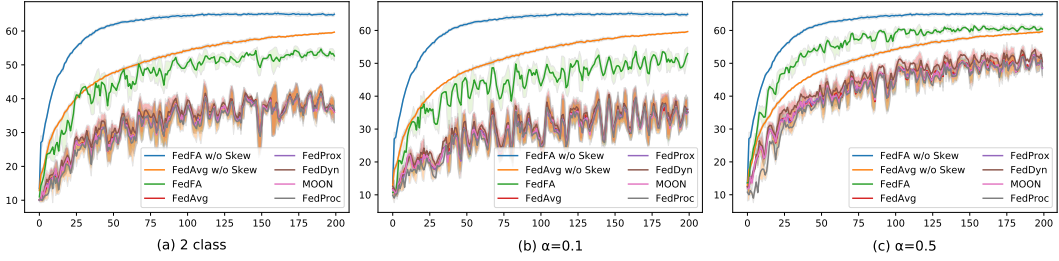


Figure 15: CIFAR-10 with label skew.

B.3.7 TRAINING ACCURACY UNDER LABEL AND FEATURE DISTRIBUTION SKEW

Figures 19 to 21 show the better performance of FedFA over all baselines under label & feature skew on Mixed Digit.

C MORE DISCUSSION

C.1 COMPARISON WITH CENTER LOSS

Our feature anchor loss borrows the idea of the center loss (Wen et al., 2016), but the purposes of these two losses are different.

- Since data heterogeneity would make gradient-based updates diverge in local training. If feature anchor loss follow gradient-based updates for feature anchors, the anchors would be harmful to align features across clients.
- Besides with a different updating method, the center loss aims to decrease the feature distance for intra-class samples in centralized training, rather than keeping feature mapping consistent across clients.
- The feature anchors are not utilized to calibrate the classifier in (Wen et al., 2016), but our work does it to prevent the divergence of classifiers across clients in federated training. For example, missing some class samples would make classifier updates diverge and contract the margin between the features corresponding to missing classes and their decision boundaries in classifiers.

Therefore, we use the feature anchor loss to distinguish the center loss proposed by the research community on face recognition.

C.2 THE BENEFIT OF FEATURE ANCHOR LOSS WITHOUT LOCAL CLASSIFIER CALIBRATION

There exist feature extractors so that the features are class-discriminative to show the property of FedFA on the mitigation of classifier divergence:

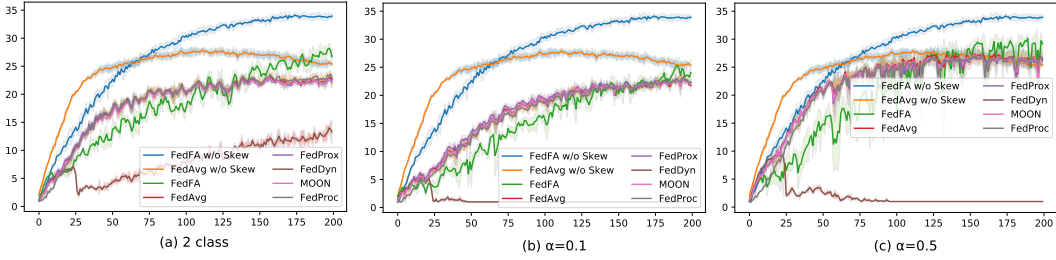


Figure 16: CIFAR-100 with label skew.

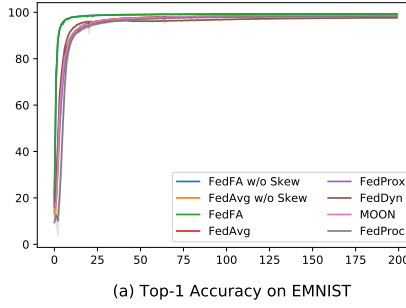


Figure 17: EMNIST with feature skew.

Assumption 1 (Discriminative features) There exist a constant δ , C sub hyperspaces $\{\mathcal{H}_c\}_{c=1}^C$ in the feature space \mathcal{H} , and C feature anchors $\{\mathbf{a}_c\}_{c=1}^C$ such that for all c -th class features \mathbf{h}_c , $\mathcal{H}_c = \{\mathbf{h}_c \mid \|\mathbf{h}_c - \mathbf{a}_c\|^2 < \delta^2\}$, where for $i \neq j$, $\mathcal{H}_i \cap \mathcal{H}_j = \emptyset$.

Theorem 4 (Similar classifier updates). Let Assumption 1 holds. For $\|\mathbf{a}_c\| > \sqrt{2}\delta$ and the inner product $\mathbf{h}_c \cdot \mathbf{h}_q \leq 0$ where $c \neq q$, $\mathbf{h}_c \in \mathcal{H}_c$ and $\mathbf{h}_q \in \mathcal{H}_q$, we have:

$$\cos(\Delta\phi_{i,c}, \Delta\phi_{v,c}) > 0. \quad (6)$$

We direct readers to Appendix G.5 for a detailed proof, where the key idea is that the dot product of inter-class features is negative. Therefore, FedFA can achieve similar updates of the t -th proxy between clients i and v even without classifier calibration to regulate classifier updates.

C.3 PRIVACY ISSUES INTRODUCED BY FEATURE ANCHORS

FedFA can provide privacy protection at the basic level with a promising performance for federated learning. Firstly, feature anchors can be fixed/without updates during federated training (i.e., the client would not aggregate any information into feature anchors, which would not bring potential privacy leakage) because of the powerful representation of neural networks. That is, the fixed anchors in FedFA specified a feature space and a classifier between clients before training. The third row of Table 4 shows better results of experiments of FedFA without feature-anchor updates than the best baseline under label and feature skewness. Therefore, there is a trade-off between privacy and generalization performance for FedFA. Secondly, FedFA only shares the feature centroid (statistic mean of features) of the changing feature under training, rather than the fully trained feature map from raw data, so the information leaked to the attacker by the feature anchor may be limited, which is verified by (Luo et al., 2021). Thirdly, since feature anchors are a component of the trained model, we argue that current approaches such as secure aggregation and differential privacy can protect data privacy against reconstruction attacks based on feature anchors. Meanwhile, the weakness of our study is the absence of an analysis of the degree of privacy leakages by feature anchors. We will further investigate it in our future work.

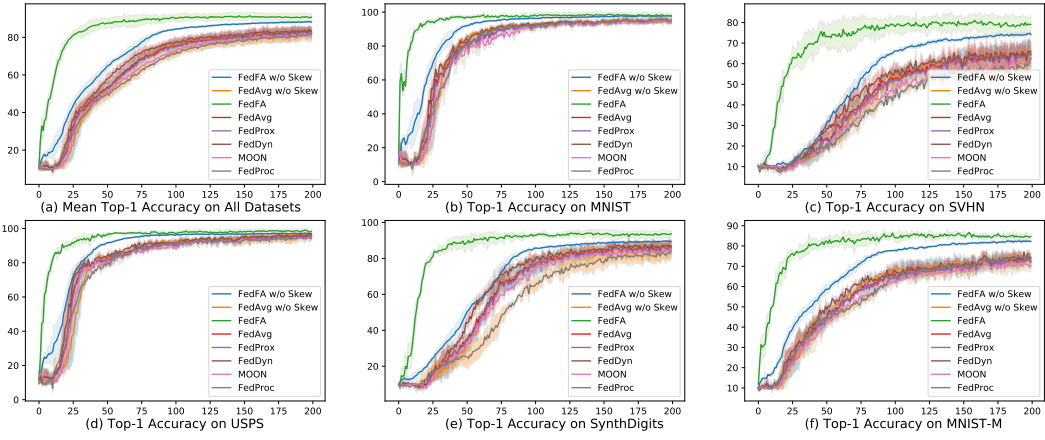


Figure 18: Mixed Digit without label skew.

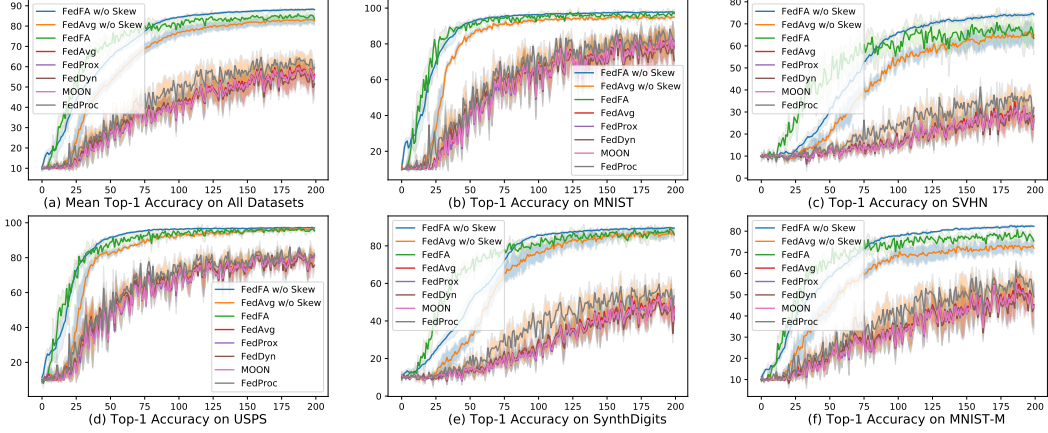


Figure 19: Mixed Digit with label skew $\#C = 2$.

C.4 CHALLENGES OF DEPLOYING CONTRASTIVE LEARNING WITH FEDERATED LEARNING

Contrastive learning is currently widely used and seeks to align sample features under various augmentations. More and more methods, such as MOON(Li et al., 2021b) and FedUFO(Zhang et al., 2021), try to solve the data heterogeneity problem from feature-contrastive perspective. One main challenge in deploying contrastive learning to federated learning is how to generate features from the datasets of other clients to perform alignment, since the privacy requirement does not allow clients to share raw data with each other. For example, MOON uses the global model to generate global features to align local features generated by local model, and our method FedFA does it by means of shared feature anchors. Moreover, another main challenge is how to balance the supervised loss and contrastive loss (an auxiliary loss) since if the contrast loss is too large at the beginning of training, it will increase the difficulty of training, but if it is too small, it will easily fail to align features.

D RELATED WORKS

Federated learning is a fast-developing area, and we mainly introduce the methods close to ours (i.e., federated optimization-based methods) and briefly introduce other methods. Comprehensive field studies have appeared in (Kairouz et al., 2021; Wang et al., 2021a; Tan et al., 2022a).

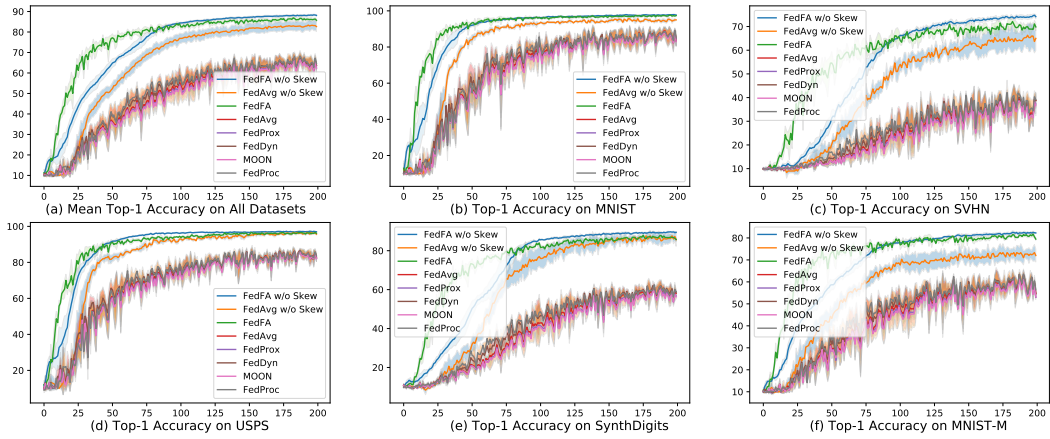


Figure 20: Mixed Digit with label skew $\alpha = 0.1$.

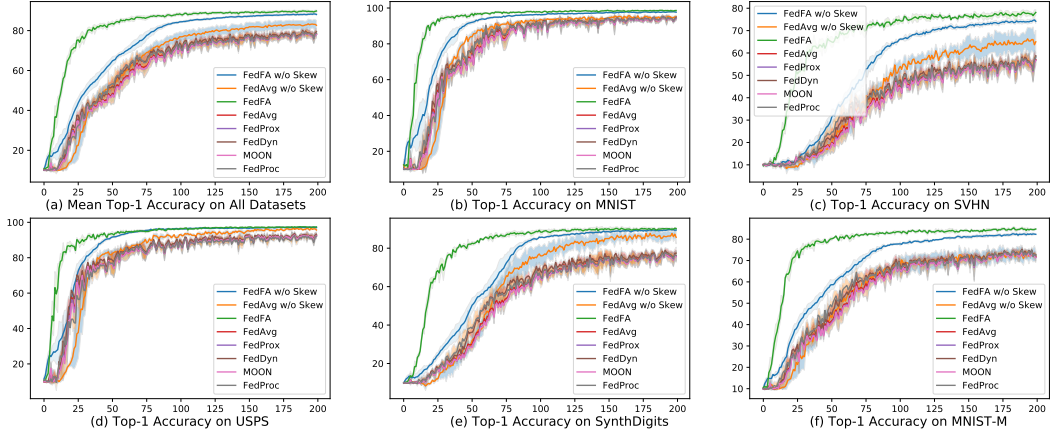


Figure 21: Mixed Digit with label skew $\alpha = 0.5$.

Tackle data heterogeneity on the client side. To avoid local models converging to their local minima instead of global minima, many works add a well-designed regularization term to penalize local models to make them not far away from the global model. For example, FedProx (Li et al., 2020) uses the Euclidean distance between local models and the global model as the regularization loss. FedDyn (Acar et al., 2021) modifies the local objective with a dynamic regularizer consisting of a linear term based on the first order condition and the Euclidean-distance term, such that the local minima are consistent with the global stationary point. MOON (Li et al., 2021b) utilizes the feature similarity between previous local models and the global model as model-contrastive regularization to correct the local training of each client. In place of the model-contrastive term in MOON, FedProc (Mu et al., 2021) introduces a prototype-contrastive term to regularize the features within each class with class prototypes (Snell et al., 2017). Besides, instead of implicit correction by regularization, a number of works reduce the bias explicitly in local updates by controlling variates or posterior sampling. Borrowing the variance-reduce technique in standard convex optimization, SCAFFOLD (Karimireddy et al., 2020) presents a control variate to correct the client updates, so they are much closer to the global update. Another way to reduce the bias is to run Markov Carlo, instead of stochastic gradient descent, which produces approximate local posterior samples like FedPA (Al-Shedivat et al., 2021). Similar to (Li et al., 2021a; Chen & Chao, 2022; Luo et al., 2021; He et al., 2021), our experiments in Section 5 show that these works may not provide stable better

performance gains over FedAvg(McMahan et al., 2017) in classification tasks, which motivates us to analyze the relationship between classifier updates and feature mappings in local training.

Tackle data heterogeneity on the server side. In addition to improving on the client side, many works have developed alternative aggregation schemes on the server side to tackle data heterogeneity. For instance, (Wang et al., 2020b) finds an objective inconsistency problem caused by unbalanced data that induces a different number of local updates and propose FedNova to eliminate the inconsistency by normalizing the local updates before averaging. Besides, (Reddi et al., 2021) adopts adaptive momentum update on the server-side to mitigate oscillation of global model updates when the server activates the clients with a limited subset of labels. Beyond layer-weighted averaging, some works like FedMA (Wang et al., 2020a) and Fed² (Yu et al., 2021) introduce neuron-wise averaging because there may exist neuron mismatching from permutation invariance of neural networks in federated learning. These ideas complement our work and can be integrated into our method because our method only adds a regularizer on the client side.

Tackle data heterogeneity based on feature. Instead of considering from the federated-optimization view, some recent works such as (Li et al., 2021b; Mu et al., 2021; Li & Zhan, 2021; Luo et al., 2021; Zhang et al., 2022; Tang et al., 2022) pay more attention to feature space across clients. To improve feature consistency, MOON (Li et al., 2021b) and FedProc (Mu et al., 2021) introduce a feature-based local regularizer mentioned above. FedUFO (Zhang et al., 2021) shares client models with each others to align features and logit output. Meanwhile, (Tang et al., 2022) generates a shared virtual dataset for all clients before training, and calibrates features by minimizing the feature distribution distance between the virtual dataset and the real dataset.

Tackle data heterogeneity based on classifier. To improve classifier consistency, (Luo et al., 2021) observes that the classifier layer (i.e., the last layer of the model) suffers most from label distribution skew and proposes calibration of the classifier with virtual features after training. Moreover, (Li & Zhan, 2021; Zhang et al., 2022) introduce a restricted loss cross-entropy and a fine-grained calibrated cross-entropy loss, respectively. The key idea of the two methods is to prevent the overfitting of missing classes (Li & Zhan, 2021) and minority classes (Zhang et al., 2022) (i.e., both under the label distribution skew) with an improved cross-entropy loss. However, compared with our method, these methods only consider the label distribution skew setting by improving the performance degeneration based on feature calibration or classifier calibration, and neglect *vicious cycle* between different classifier updates and inconsistent features, which hurts their performance.

Other methods. The data-centric method is one recent new direction, which shares common datasets with all clients like the public dataset in (Zhao et al., 2018). To avoid violating the privacy requirement, some works focus on sharing synthesized data like (Luo et al., 2021; Li et al., 2022; Tang et al., 2022) and coded data (Sun et al., 2022; Shao et al., 2022) with privacy protection to construct a more homogeneous dataset for federated learning. Moreover, another line of research aims to train a personalized model for each client, rather than a global model (Tan et al., 2022a). Since there is still no standard approach to personalized federated learning, many researchers achieve it by personalized regularization (T Dinh et al., 2020), meta learning (Fallah et al., 2020), prototype learning (Tan et al., 2022b) and personalized layers (Chen & Chao, 2022), etc.

Our work aims at the typical federated learning (McMahan et al., 2017) and tries to improve the local optimization by feature alignment in federated optimization. There are two existing works similar to ours, i.e., MOON (Li et al., 2021b) which introduces a model-contrastive loss to maximize the agreement of the features extracted by the local model and that by the global model, and FedProc (Mu et al., 2021) which proposes a prototype-contrastive loss to correct features by class prototypes. However, compared with our method, although considering the feature mapping inconsistency across local models, MOON and FedProc neglect the *vicious cycle* between different classifiers’ updates and inconsistent features, which hurts their performance.

E DETAILS OF EXPERIMENT SETUP

E.1 SPECIFIC MODELS

Our validation and test experiments, including label distribution skew, feature distribution skew and label & feature distribution skews, use the models according to Table 8. Herein, to ablate the

effect of BN layers, we follow (Hsieh et al., 2020) to replace the BN layer with the GroupNorm layer in all experiments. For a fair comparison, our models follow those reported in the baselines’ works. Specifically, following (Acar et al., 2021), we use a CNN model for EMNIST, FMNIST, and CIFAR-10, consisting of two 5x5 convolution layers followed by 2x2 max pooling and two fully-connected layers with ReLU activation. Following (Li et al., 2021b) and (Li et al., 2021c), we utilize the ResNet-18 (He et al., 2016) with a linear projector for CIFAR-100 and a CNN model with three 5x5 convolution layers followed by five GroupNorm layers for the Mixed Digits dataset.

Table 8: The specific parameters settings for all the models used in our experiments.

Layer	Validation Experiment		Test Experiment		
	Label Skew	Feature Skew	Label Skew	CIFAR-100	Feature Skew
	FMNIST	Mixed-digit dataset	FMNIST/EMNIST	CIFAR-10	Mixed-digit dataset
1	Conv2d(1, 32, 5) ReLU,MaxPool2D(2,2)	Conv2d(3, 64, 5) ReLU,MaxPool2D(2,2)	Conv2d(1, 32, 5) ReLU,MaxPool2D(2,2)	Conv2d(3, 64, 5) ReLU,MaxPool2D(2,2)	Basicbone of Resnet18 with GroupNorm ReLU,MaxPool2D(2,2)
2	Conv2d(32, 32, 5) ReLU,MaxPool2D(2,2)	Conv2d(64, 64, 5) ReLU,MaxPool2D(2,2)	Conv2d(32, 32, 5) ReLU,MaxPool2D(2,2)	Conv2d(64, 64, 5) ReLU, MaxPool2D(2,2)	FC(512,512) ReLU Conv2d(64, 64, 5, 1, 2) ReLU,MaxPool2D(2,2)
3	FC(992,384) ReLU	FC(1024,384) ReLU	FC(992,384) ReLU	FC(1600,384) ReLU	FC(512,256) Conv2d(3, 128, 5, 1, 2) ReLU
4	FC(384,100)	FC(384,100)	FC(384,192) ReLU	FC(384,192) ReLU	FC(256,100) FC(6272, 2048) ReLU
5	FC(100,10)	FC(100,10)	FC(192,10)	FC(192,10)	FC(2048,512) ReLU
6					FC(512,10)
Source			model from (Acar et al., 2021)	model from (Acar et al., 2021)	model from (Li et al., 2021b)
					model from (Li et al., 2021c)

E.2 VALIDATION EXPERIMENT SETUP

The total number of training samples per client is 1000 in this case. We separately sample a subset from test sets of FMNIST and Mixed Digit to visualize the normalized feature mappings of the local models based on t-SNE visualization (Van der Maaten & Hinton, 2008). In Figure 2, although we input the same Validation samples into all clients’ local modes, we only show their features mappings for which clients have the corresponding class (i.e., if client 1 only holds class 1 and class 2 samples, we only offer the feature maps of the client 1 model for these two classes, as it would be unfair to ask the local model of client 1 to map the feature of classes on which it did not learn.). We visualize the feature mappings of client models according to the labels (digit dataset) owned by the corresponding client for label (distribution) skew. The specific setup is described as:

- **Label Distribution Skew:** The experiment has 10 clients where each client has 2 classes with 500 samples per class from FMNIST, and utilizes the SGD optimizer with a 0.01 learning rate and without momentum. The federated setting involves 10 local epoch numbers, 15 communication rounds, and a 100% client sample rate. The top-1 accuracy of global model of all method at the targeted communication round is that FedAvg without skew: 80.32%; FedAvg:52.66%; FedProx:51.43%; FedDyn:51.90%; MOON:45.67%; FedProc:49.87%; FedFA(our): 67.54%.
- **Feature Distribution Skew:** The experiment has 10 clients where each client has 10 classes with 100 samples per class from one of the digit datasets in Mixed Digit (i.e., MNIST, SVHN, USPS, SynthDigits, and MNIST-M), and utilizes the SGD optimizer with a 0.01 learning rate and without momentum. The federated setting involves 10 local epoch numbers, 15 communication rounds, and a 100% client sample rate. The Mean top-1 accuracy of the global models of all methods at the targeted communication round is that FedAvg without skew: 81.66%; FedAvg:79.56%; FedProx:78.76%; FedDyn:79.60%; MOON: 79.58%; FedProc:79.30%; FedFA(our): 80.44%.

E.3 TEST EXPERIMENT SETUP

Baselines. Federated learning (McMahan et al., 2017) aims to train a global model parameterized by \mathbf{w} by collaborating a total of N clients with a central server to solve the following optimization problem:

$$\min_{\mathbf{w} \in \mathbb{R}^d} \mathcal{L}(\mathbf{w}) := \mathbb{E}_i[\mathcal{L}_i(\mathbf{w})] = \sum_i^N \frac{n_i}{n} \mathcal{L}_i(\mathbf{w})$$

where $n = \sum_i n_i$ represents the total sample size with n_i being the sample size of the i -th client, and $\mathcal{L}_i(\mathbf{w}) := \mathbb{E}_{\xi \in \mathcal{D}_i} [l_i(\mathbf{w}; \xi)]$ is the local objective function in local dataset \mathcal{D}_i of the i -th client.

Many methods have been proposed to solve this optimization problem and alleviate the negative impact of data heterogeneity across clients. Herein, from the view of local-optimization methods, we compare FedFA with the common federated learning algorithms, including FedAvg(McMahan et al., 2017), FedProx(Li et al., 2020) and the state-of-the-art methods based on well-designed local regularization including FedDyn (Acar et al., 2021), MOON (Li et al., 2021b) and FedProc (Mu et al., 2021). The specific description of these methods can be denoted as:

- **FedAvg:** As a canonical method to solve (1) proposed by (McMahan et al., 2017), in each communication round, FedAvg firstly selects a subset of clients and initiates client models as \mathbf{w} and then updates the local models \mathbf{w}_i by minimizing $\mathcal{L}_i(\mathbf{w})$, and finally aggregates the local models \mathbf{w}_i as the new global model \mathbf{w} until $\mathcal{L}(\mathbf{w})$ arrives at a stationary point.
- **FedProx:** FedProx (Li et al., 2020) adds the Euclidean regularization loss between local models and the global model in the local optimization problem, which can be described as:

$$\mathcal{L}_i(\mathbf{w}) = \min_{\mathbf{w}_i} \mathbb{E}_{(\mathbf{x}, y) \in \mathcal{D}_i} [l_i(\mathbf{w}_i; \mathbf{w}^{(t-1)}) + \frac{\mu}{2} \|\mathbf{w}_i - \mathbf{w}^{(t-1)}\|^2]. \quad (7)$$

- **FedDyn:** FedDyn (Acar et al., 2021) modifies the local objective with a dynamic regularization consisting of a linear term based on the first order condition and an above Euclidean-distance term, such that the local minima are consistent with the global stationary point, which can be described as:

$$\mathcal{L}_i(\mathbf{w}) = \min_{\mathbf{w}_i} \mathbb{E}_{(\mathbf{x}, y) \in \mathcal{D}_i} [l_i(\mathbf{w}_i; \mathbf{w}^{(t-1)}) - \langle \nabla \mathcal{L}_i(\mathbf{w}^{(t-1)}), \mathbf{w}_i \rangle + \frac{\mu}{2} \|\mathbf{w}_i - \mathbf{w}^{(t-1)}\|^2]. \quad (8)$$

- **MOON:** MOON (Li et al., 2021b) utilizes the feature similarity of the client model with previous-round local models and with the global model as model-contrastive regularization to correct the local training of each client, which can be described as:

$$\mathcal{L}_i(\mathbf{w}) = \min_{\mathbf{w}_i} \mathbb{E}_{(\mathbf{x}, y) \in \mathcal{D}_i} [l_i(\mathbf{w}_i; \mathbf{w}^{(t-1)}) - \mu \log \frac{\exp(sim(\mathbf{h}_i, \mathbf{h}_{\text{global}})/\tau)}{\exp(sim(\mathbf{h}_i, \mathbf{h}_{\text{global}})/\tau) + \exp(sim(\mathbf{h}_i, \mathbf{h}_{\text{pre}})/\tau)}] \quad (9)$$

where \mathbf{h}_i , $\mathbf{h}_{\text{global}}$, \mathbf{h}_{pre} denote the feature mappings of the local model \mathbf{w}_i , the global model \mathbf{w} , and the local model at previous round \mathbf{w}_i^{t-1} given the same input \mathbf{x} , respectively; τ is the hyperparameter to control the effect of cosine similarity in model-contrastive loss.

- **FedProc:** Instead of the model-contrastive term in MOON, FedProc (Mu et al., 2021) introduces a prototype-contrastive term to regularize the features within each class with class prototypes (Snell et al., 2017), which can be described as:

$$\mathcal{L}_i(\mathbf{w}) = \min_{\mathbf{w}_i} \mathbb{E}_{(\mathbf{x}, y) \in \mathcal{D}_i} [\frac{t}{T} l_i(\mathbf{w}_i; \mathbf{w}^{(t-1)}) + (1 - \frac{t}{T}) \log \frac{\exp(sim(\mathbf{h}_i, \mathbf{p}_c)/\tau)}{\sum_{c=1}^C \exp(sim(\mathbf{h}_i, \mathbf{p}_c)/\tau)}] \quad (10)$$

where T is the targeted communication round, and \mathbf{p}_c is the prototype of class c . In FedProc, \mathbf{p}_c is updated by the whole local dataset at the end of one communication round (i.e., $\mathbf{p}_{c,i}^{(t,k)} = \frac{1}{|\mathcal{D}_{i,c}|} \sum_{(\mathbf{x}, c) \in \mathcal{D}_{i,c}} \mathbf{h}_{i,c}$). However, we need to denote that if \mathbf{p}_c is updated like this, rather than the momentum update as ours and we found that FedProc would suffer from the divergence because the update of \mathbf{p}_c is too drastic in our experiments¹. Therefore, we improve FedProc with our momentum update.

Datasets. This work aims at image classification tasks under label distribution skew, feature distribution skew and label & feature distribution skew, and uses benchmark datasets with the same data heterogeneity setting as (McMahan et al., 2017; Yurochkin et al., 2019; Li et al., 2021a), including EMNIST(Cohen et al., 2017), FMNIST(Xiao et al., 2017), CIFAR-10, CIFAR-100 (Krizhevsky et al., 2009), and Mixed Digits dataset (Li et al., 2021c). Specifically, for label distribution skew, we consider two settings:

¹The codes of FedProc are not open source, and thus our reproduction settings cannot be completely consistent to the original setting, but we fine-tune the hyperparameter of FedProc carefully and report the best results.

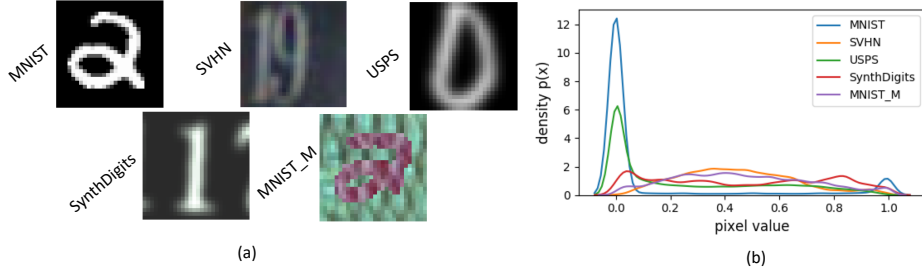


Figure 22: Data visualization. (a) Examples from each dataset (client) in Mixed Digit. (b) feature distributions skew across the datasets (over random 100 samples for each dataset).

- **Same size of local dataset:** Following (McMahan et al., 2017), we split data samples based on classes to clients (e.g., $\#C = 2$ denotes each client holds two class samples), where each client holds 250 samples per class;
- **Different sizes of local dataset:** Following (Yurochkin et al., 2019), we first sample p_i from Dirichlet distribution $Dir(\alpha)$ and then assign $p_{i,c}$ proportion of the samples of class c to client i , where we set α as 0.1 and 0.5 to measure the the level of data heterogeneity in our experiments. Moreover, when $\alpha = 0.1$, the label distributions across clients are so skewed that the quantity of clients' local dataset is also skewed. That is, the experiment cases related to $\alpha = 0.1$ would involve label distribution skew and quantity distribution skew, which denotes the unbalanced data size of the local dataset across clients.

For feature distribution skew, we consider two settings:

- **Real-world feature imbalance:** We use a subset of the real-world dataset with natural feature imbalance, EMNIST(Cohen et al., 2017), including 10 classes and 341873 samples (about 34000 samples per class) totally;
- **Artificial feature imbalance:** We use a mixed-digit dataset from (Li et al., 2021c) consisting of five benchmark digit datasets: MNIST(LeCun et al., 1998), SVHN(Netzer et al., 2011), USPS(Hull, 1994), SynthDigits and MNIST-M(Ganin et al., 2015), including 7430 samples for one digit dataset and 743 sample per class. The data visualization is shown as Figure 22².

Note that for the experiments on Mixed Digits, we report the average top-1 accuracy on five benchmark digit datasets in Table 2 and Table 4, and show the top-1 accuracy on each digit dataset during the training in Figure 18 to Figure 20. For the experiments on other datasets except for Mixed Digits, we test the top-1 accuracy on all datasets based on the global model and report them during the training as shown in Figure 14 to Figure 17.

Federated Simulation Setup. All experiments are performed based on PyTorch Paszke et al. (2019) and one node of the High-Performance Computing platform with 4 NVIDIA A30 Tensor Core GPUs with 24GB. We use an existing dataset-split tool FedLab (Zeng et al., 2021) to generate federated local datasets for all clients. There are in total 100 clients, and 10 clients participating in federated training at each communication round. We use the SGD optimizer with a 0.01 learning rate and 0.001 weight decay for all experiments except for the CIFAR-100 experiment, which uses 0.9 momentum additionally. The local batch size is 64, the number of local epochs is set to 5, and the number of communication rounds is set to 200. Moreover, we carefully select the coefficient of local regularization from $\{1, 0.1, 0.01\}$ (i.e., $\mu/2 = 0.05$ for FedProx and FedDyn, $\mu = 1$ for MOON except $\mu = 5$ on CIFAR-10), set the temperature hyperparameter $\tau = 0.5$ for MOON and FedProc, and report their best results in our experiments.

FedFA setup. We set the coefficient of exponential moving average $\lambda = 0.5$ in momentum accumulation for feature anchors in local training and local loss coefficient $\mu = 0.1$ in (4) like our baselines, and according to Property 4, we initiate the pairwise orthogonal feature anchors \mathbf{a}_c by

²Figure comes from(Li et al., 2021c)

sampling column vector from an identity matrix whose dimension is the same as the size of the feature mappings. Other settings of FedFA are the same as baselines in all experiments, such as the same random seed (seed: 2021, 2022, 2023) and the same training and test dataset.

F PSEUDOCODE OF FEDFA

At the local update of FedFA, client i does not update $\mathbf{a}_c^{(t-1)}$, but accumulate the c -th class features of the τ -th batch $\mathcal{B}_i^{(t,k_\tau)}$ as:

$$\mathbf{m}_{c,i}^{(t,k_\tau)} = \mathbf{m}_{c,i}^{(t,k_{\tau-1})} + \frac{1}{B|\mathcal{B}_{i,c}^{(t,k_\tau)}|} \sum_{(\mathbf{x},c) \in \mathcal{B}_{i,c}^{(t,k_\tau)}} f_{\boldsymbol{\theta}_i}(\mathbf{x}) \quad (11)$$

where B represents the total mini-batch number of one epoch and $\mathbf{m}^{(t,k_0)} = 0$. Herein, to reduce computation, we take each epoch momentum $\mathbf{m}_{c,i}^{(t,k)}$ to estimate the class features by

$$\bar{\mathbf{a}}_{c,i}^{(t,k)} = \lambda \mathbf{m}_{c,i}^{(t,k-1)} + (1 - \lambda) \mathbf{m}_{c,i}^{(t,k)} \quad (12)$$

instead of computing them with training dataset after local training.

The pseudocode of FedFA is shown as the following Algorithm 1. Compared with FedAvg, FedFA adds a feature anchor loss and calibrates the classifier locally.

Algorithm 1 FedFA (Proposed Framework): Federated Learning with Feature Anchors

Input: initial model $\mathbf{w} = \{\boldsymbol{\theta}, \boldsymbol{\phi}\}$, initial feature anchors $\{\mathbf{a}_c\}_{c=1}^C$, learning rate η , local epoch K , client number N , class number C

for each round $t = 1, \dots, R$ **do**

- Server samples clients $\mathcal{S} \subseteq \{1, \dots, N\}$
- Server communicates $\mathbf{w}^{(t-1)}$ and $\{\mathbf{a}_c^{(t-1)}\}_{c=1}^C$ to all clients $i \in \mathcal{S}$
- on client $i \in \mathcal{S}$ in parallel do**

 - Initialize the local model $\mathbf{w}_i \leftarrow \mathbf{w}^{(t-1)}$, the local feature anchor $\mathbf{a}_{c,i} \leftarrow \mathbf{a}_c^{(t-1)}$
 - for** local epoch $k = 1, \dots, K$ **do**

 - for** each mini-batch **do**

 - % feature alignment with feature anchors
 - Calculate the local loss $l_i \leftarrow l_{\text{sup}_i} + \mu l_{\text{fa}_i}$ according to (4)
 - Compute mini-batch gradient $g_i(\mathbf{w}_i) \leftarrow \nabla_{\mathbf{w}_i} l_i$
 - Update local model $\mathbf{w}_i \leftarrow \mathbf{w}_i - \eta g_i(\mathbf{w}_i)$
 - % classifier calibration with feature anchors
 - Calculate the calibration loss $l_i \leftarrow l_{\text{cal}_i}$ according to (5)
 - Compute mini-batch gradient $g_i(\boldsymbol{\phi}_i) \leftarrow \nabla_{\boldsymbol{\phi}_i} l_{\text{cal}_i}$
 - Calibrate classifier proxies $\boldsymbol{\phi}_i \leftarrow \boldsymbol{\phi}_i - \eta g_i(\boldsymbol{\phi}_i)$
 - % Accumulate class features
 - Perform moving average to estimate the expectation of feature anchors according to (11)
 - Estimate feature anchors $\mathbf{m}_i^{(t,k)}$ according to (12)

 - end for**
 - Communicate $\mathbf{w}_i^{(t)}$ and $\{\mathbf{a}_{c,i}^{(t)}\}_{c=1}^C$ back to the server

 - end on client**
 - Server aggregates the global model $\mathbf{w}^{(t)} \leftarrow \frac{1}{|\mathcal{S}|} \sum_{i \in \mathcal{S}} \mathbf{w}_i^{(t)}$, and the feature anchors $\mathbf{a}_c^{(t)} \leftarrow \frac{1}{|\mathcal{S}|} \sum_{i \in \mathcal{S}} \mathbf{a}_{c,i}^{(t)}$ according to weighted aggregation
 - end for**

G PROOF

G.1 PROOF OF DEFINITION (1)

Proof 1 (Proof of Definition 1) According to the gradient of cross entropy loss, we have:

$$\begin{aligned}
\Delta_{\phi_c}^{a,b} &= \Delta\phi_{a,c} - \Delta\phi_{b,c} \\
&= \underbrace{\left(\frac{\eta}{n_a} \sum_{y_j=c}^{n_{a,c}} (1 - p_{a,c}^{(j)}) \mathbf{h}_{a,y_j} - \frac{\eta}{n_b} \sum_{y_j=c}^{n_{b,c}} (1 - p_{b,c}^{(j)}) \mathbf{h}_{b,y_j} \right)}_{\text{mean deviation by positive features}} \\
&\quad - \underbrace{\left(\frac{\eta}{n_a} \sum_{y_j \neq c}^{n_a - n_{a,c}} p_{a,c}^{(j)} \mathbf{h}_{a,y_j} - \frac{\eta}{n_b} \sum_{y_j \neq c}^{n_a - n_{b,c}} p_{b,c}^{(j)} \mathbf{h}_{b,y_j} \right)}_{\text{mean deviation by negative features}} \\
&\approx \left(\frac{\eta n_{a,c}}{n_a} \left(1 - \overline{p_{a,c}^{(c)}} \right) \bar{\mathbf{h}}_{a,c} - \frac{\eta n_{b,c}}{n_b} \left(1 - \overline{p_{b,c}^{(c)}} \right) \bar{\mathbf{h}}_{b,c} \right) \quad (13) \\
&\quad - \left(\frac{\eta}{n_a} \sum_{\bar{c}_a \neq c} n_{a,\bar{c}_a} \overline{p_{a,\bar{c}_a}^{(\bar{c}_a)}} \bar{\mathbf{h}}_{a,\bar{c}_a} - \frac{\eta}{n_b} \sum_{\bar{c}_b \neq c} n_{b,\bar{c}_b} \overline{p_{b,\bar{c}_b}^{(\bar{c}_b)}} \bar{\mathbf{h}}_{b,\bar{c}_b} \right) \\
&\stackrel{n_b=n}{=} \frac{\eta}{n} \underbrace{\left[\left(n_{a,c} \left(1 - \overline{p_{a,c}^{(c)}} \right) \bar{\mathbf{h}}_{a,c} - n_{b,c} \left(1 - \overline{p_{b,c}^{(c)}} \right) \bar{\mathbf{h}}_{b,c} \right)}_{\text{mean deviation by positive features}} \\
&\quad - \underbrace{\left(\sum_{\bar{c}_a \neq c} n_{a,\bar{c}_a} \overline{p_{a,\bar{c}_a}^{(\bar{c}_a)}} \bar{\mathbf{h}}_{a,\bar{c}_a} - \sum_{\bar{c}_b \neq c} n_{b,\bar{c}_b} \overline{p_{b,\bar{c}_b}^{(\bar{c}_b)}} \bar{\mathbf{h}}_{b,\bar{c}_b} \right)}_{\text{deviation by mean negative features}} \right]
\end{aligned}$$

where the term of “ \approx ” holds from Property 1 in (Zhang et al., 2022) based on the statistic results of Figures 4 and 5 in Appendix of (Wang et al., 2021b) (i.e., it is practical for the feature extraction of one client to assume $\overline{p_{\cdot,c}^{(c)}} \bar{\mathbf{h}}_{\cdot,c} = \frac{1}{n_{\cdot,c}} \sum_{y_j=c}^{n_{\cdot,c}} p_{\cdot,c}^{(j)} \mathbf{h}_{\cdot,y_j}$ where $\overline{p_{\cdot,c}^{(c)}} = \frac{1}{n_{\cdot,c}} \sum_{y_j=c}^{n_{\cdot,c}} p_{\cdot,c}^{(j)}$ and $\bar{\mathbf{h}}_{\cdot,c} = \frac{1}{n_{\cdot,c}} \sum_{y_j=c}^{n_{\cdot,c}} \mathbf{h}_{\cdot,y_j}$). It should be noted that we do not assume that the extracted features of the same class across clients are similar (i.e., $\bar{\mathbf{h}}_{a,c} \neq \bar{\mathbf{h}}_{b,c}$) like (Wang et al., 2021b), which is also verified by the histograms of Figure 5 to 8.

G.2 PROOF OF THEOREM (1)

Observation 3 From our empirical study where client models would be given the same class samples to extract features if their datasets have the same class, the histograms of Figures 5 to 8 show that the cos-similarity peaks of positive and negative pairs do not overlap, which indicates that the class features are class-discriminative across clients.

With observation 3, it is practical for us to assume:

Assumption 2 The mean class feature $\bar{\mathbf{h}}_{\cdot,c_1} \neq \alpha \bar{\mathbf{h}}_{\cdot,c_2}$ if $c_1 \neq c_2$ across clients. Meanwhile, clients would hold the same samples if their datasets have the same class.

Proof 2 (Proof of Theorem 1) For label distribution skew, we consider the classifier update divergence between client a and client b when $[C_a] \neq [C_b]$.

When $c \in [C_a] \cap [C_b]$, $\bar{\mathbf{h}}_{a,c} = \bar{\mathbf{h}}_{b,c}$, $\overline{p_{a,c}^{(c)}} = \overline{p_{b,c}^{(c)}}$ and the deviation by mean positive features $\Delta_{\phi_c}^{(+)_a,b} = 0$, and then we have:

$$\begin{aligned} \|\Delta_{\phi_c}^{a,b}\|^2 &= \frac{\eta^2}{n^2} \|\Delta_{\phi_c}^{(-)_a,b}\|^2 = \frac{\eta^2}{n^2} \left\| \sum_{\bar{c}_a \neq c} n_{a,\bar{c}_a} \overline{p_{a,c}^{(\bar{c}_a)}} \bar{\mathbf{h}}_{a,\bar{c}_a} - \sum_{\bar{c}_b \neq c} n_{b,\bar{c}_b} \overline{p_{b,c}^{(\bar{c}_b)}} \bar{\mathbf{h}}_{b,\bar{c}_b} \right\|^2 \\ &= \frac{\eta^2}{n^2} \left\| \sum_{\hat{c}_a} n_{a,\hat{c}_a} \overline{p_{a,c}^{(\hat{c}_a)}} \bar{\mathbf{h}}_{a,\hat{c}_a} - \sum_{\hat{c}_b} n_{b,\hat{c}_b} \overline{p_{b,c}^{(\hat{c}_b)}} \bar{\mathbf{h}}_{b,\hat{c}_b} \right\|^2 \\ &> 0 \end{aligned} \quad (14)$$

where $\hat{c}_a \in [C_a] \setminus \{[C_a] \cap [C_b]\}$ and $\hat{c}_b \in [C_b] \setminus \{[C_a] \cap [C_b]\}$ (i.e., \hat{c}_a denotes the classes for which client a has samples in its dataset but client b does not). If the equality of (14) holds, $\bar{\mathbf{h}}_{a,\hat{c}_a} = \alpha \bar{\mathbf{h}}_{b,\hat{c}_b}$ where $\alpha = n_{a,\hat{c}_a} \overline{p_{a,c}^{(\hat{c}_a)}} / n_{b,\hat{c}_b} \overline{p_{b,c}^{(\hat{c}_b)}}$, but this is a contradiction to Assumption 2 and Observation 3. Thus, classifier updates between client a and client b would be diverged when $c \in [C_a] \cap [C_b]$.

When $c \in \{[C] \setminus \{[C_a] \cup [C_b]\}\}$, $n_{a,c} = n_{b,c} = 0$ and $\Delta_{\phi_c}^{(+)_a,b} = 0$, and then we have:

$$\begin{aligned} \|\Delta_{\phi_c}^{a,b}\|^2 &= \frac{\eta^2}{n^2} \|\Delta_{\phi_c}^{(-)_a,b}\|^2 = \frac{\eta^2}{n^2} \left\| \sum_{\bar{c}_b \in [C_b]} n_{b,\bar{c}_b} \overline{p_{b,c}^{(\bar{c}_b)}} \bar{\mathbf{h}}_{b,\bar{c}_b} - \sum_{\bar{c}_a \in [C_a]} n_{a,\bar{c}_a} \overline{p_{a,c}^{(\bar{c}_a)}} \bar{\mathbf{h}}_{a,\bar{c}_a} \right\|^2 \\ &= \frac{\eta^2}{n^2} \left\| \sum_{\hat{c}_a} n_{a,\hat{c}_a} \overline{p_{a,c}^{(\hat{c}_a)}} \bar{\mathbf{h}}_{a,\hat{c}_a} - \sum_{\hat{c}_b} n_{b,\hat{c}_b} \overline{p_{b,c}^{(\hat{c}_b)}} \bar{\mathbf{h}}_{b,\hat{c}_b} \right\|^2 \\ &> 0 \end{aligned} \quad (15)$$

where the inequality holds because $[C_a] \neq [C_b]$ and the second row of term “ = ” is the same as (14). Thus, there exists classifier updates divergence between client a and client b when $c \in \{[C] \setminus \{[C_a] \cup [C_b]\}\}$.

When $c \in [C_a] \setminus \{[C_a] \cap [C_b]\}$, $n_{b,c} = 0$, and then we have:

$$\begin{aligned} \|\Delta_{\phi_c}^{a,b}\|^2 &= \frac{\eta^2}{n^2} \|\Delta_{\phi_c}^{(+)_a,b} - \Delta_{\phi_c}^{(-)_a,b}\|^2 \\ &= \frac{\eta^2}{n^2} \|n_{a,c} \left(1 - \overline{p_{a,c}^{(c)}}\right) \bar{\mathbf{h}}_{a,c} - \Delta_{\phi_c}^{(-)_a,b}\|^2 \\ &= \frac{\eta^2}{n^2} \|n_{a,c} \left(1 - \overline{p_{a,c}^{(c)}}\right) \bar{\mathbf{h}}_{a,c} - \left(\sum_{\bar{c}_a \neq c} n_{a,\bar{c}_a} \overline{p_{a,c}^{(\bar{c}_a)}} \bar{\mathbf{h}}_{a,\bar{c}_a} - \sum_{\bar{c}_b \neq c} n_{b,\bar{c}_b} \overline{p_{b,c}^{(\bar{c}_b)}} \bar{\mathbf{h}}_{b,\bar{c}_b} \right)\|^2 \\ &= \frac{\eta^2}{n^2} \|n_{a,c} \bar{\mathbf{h}}_{a,c} + \sum_{\hat{c}_b} n_{b,\hat{c}_b} \overline{p_{b,c}^{(\hat{c}_b)}} \bar{\mathbf{h}}_{b,\hat{c}_b} - \sum_{\hat{c}_a} n_{a,\hat{c}_a} \overline{p_{a,c}^{(\hat{c}_a)}} \bar{\mathbf{h}}_{a,\hat{c}_a}\|^2 \\ &\approx \frac{\eta^2}{n^2} \|n_{a,c} \bar{\mathbf{h}}_{a,c} - \overline{p_{a,c}^{(c)}} \bar{\mathbf{h}}_{a,c}\| \\ &> 0 \end{aligned} \quad (16)$$

where the equality holds if and only if $\Delta_{\phi_c}^{(-)_a,b} = n_{a,c} \left(1 - \overline{p_{a,c}^{(c)}}\right) \bar{\mathbf{h}}_{a,c}$. During training, it is quite challenging to maintain this situation between any two clients, so the term of “ \approx ” is because $\overline{p_{a,c}^{(\bar{c})}} \ll \overline{p_{a,c}^{(c)}} < 1$, so we can say that $\|\Delta_{\phi_c}^{a,b}\|^2$ is much more likely to be positive. The case of $c \in [C_b] \setminus \{[C_a] \cap [C_b]\}$ is the same at that of $c \in [C_a] \setminus \{[C_a] \cap [C_b]\}$. We would not discuss this case herein. Thus, there exists classifier updates divergence between client a and client b when $c \in \{[C] \setminus \{[C_a] \cup [C_b]\}\}$ or $c \in [C_b] \setminus \{[C_a] \cap [C_b]\}$.

For feature distribution skew, client a and client b share the feature extractor at the start of each round, the skewed input features of samples induce the client models to map inconsistent features (i.e., $\bar{\mathbf{h}}_{a,c} \neq \bar{\mathbf{h}}_{b,c}$), and we have:

$$\|\Delta_{\phi_c}^{a,b}\|^2 = \frac{\eta^2}{n^2} \|\Delta_{\phi_c}^{(+)_a,b} - \Delta_{\phi_c}^{(-)_a,b}\|^2 \geq \frac{\eta^2}{n^2} \left| \|\Delta_{\phi_c}^{(+)_a,b}\|^2 - \|\Delta_{\phi_c}^{(-)_a,b}\|^2 \right| \geq 0. \quad (17)$$

where the equality holds if and only if $\|\Delta_{\phi_c}^{(+),a,b}\|^2 = \|\Delta_{\phi_c}^{(-),a,b}\|^2$, but due to $\bar{\mathbf{h}}_{a,c} \neq \bar{\mathbf{h}}_{b,c}$, it is quite challenging to maintain this situation between any two clients during training. Thus, we can say that $\|\Delta_{\phi_c}^{a,b}\|^2 > 0$.

In conclusion, both label skew and feature skews diverge the classifier updates across clients.

G.3 PROOF OF DEFINITION 2

Proof 3 (Proof of Definition 2 and Theorem 2) According to the gradient of cross entropy loss, we have:

$$\begin{aligned}
\Delta_{\mathbf{h}_c}^{a,b} &= \Delta\bar{\mathbf{h}}_{a,c} - \Delta\bar{\mathbf{h}}_{b,c} \\
&= \underbrace{\frac{\eta}{n} \sum_{y_j=c} \left[\underbrace{\left((1 - p_{a,c}^{(y_j)})\phi_{a,c} - (1 - p_{b,c}^{(y_j)})\phi_{b,c} \right)}_{\text{deviation by positive classifier proxy}} - \underbrace{\left(\sum_{\bar{c}} p_{a,\bar{c}}^{(y_j)} \phi_{a,\bar{c}} - \sum_{\bar{c}} p_{b,\bar{c}}^{(y_j)} \phi_{b,\bar{c}} \right)}_{\text{deviation by negative classifier proxies}} \right]}_{\text{mean deviation by positive classifier proxy: } \Delta_{\mathbf{h}_c}^{(+),a,b}} \\
&= \frac{\eta}{n} \left[\left(\sum_{y_j=c} (1 - p_{a,c}^{(y_j)})\phi_{a,c} - \sum_{y_j=c} (1 - p_{b,c}^{(y_j)})\phi_{b,c} \right) - \left(\sum_{y_j=c} \sum_{\bar{c}} p_{a,\bar{c}}^{(y_j)} \phi_{a,\bar{c}} - \sum_{y_j=c} \sum_{\bar{c}} p_{b,\bar{c}}^{(y_j)} \phi_{b,\bar{c}} \right) \right] \\
&= \frac{\eta}{n} \left[\left(n_{a,c} (1 - \overline{p_{a,c}^{(c)}}) \phi_{a,c} - n_{b,c} (1 - \overline{p_{b,c}^{(c)}}) \phi_{b,c} \right) - \left(\sum_{\bar{c}} n_{a,c} \overline{p_{a,\bar{c}}^{(c)}} \phi_{a,\bar{c}} - \sum_{\bar{c}} n_{b,c} \overline{p_{b,\bar{c}}^{(c)}} \phi_{b,\bar{c}} \right) \right] \\
&= \eta \left[\underbrace{\left((1 - \overline{p_{a,c}^{(c)}}) \phi_{a,c} - (1 - \overline{p_{b,c}^{(c)}}) \phi_{b,c} \right)}_{\text{mean deviation by positive classifier proxy: } \Delta_{\mathbf{h}_c}^{(+),a,b}} - \underbrace{\left(\sum_{\bar{c}} \overline{p_{a,\bar{c}}^{(c)}} \phi_{a,\bar{c}} - \sum_{\bar{c}} \overline{p_{b,\bar{c}}^{(c)}} \phi_{b,\bar{c}} \right)}_{\text{mean deviation by negative classifier proxies: } \Delta_{\mathbf{h}_c}^{(-),a,b}} \right] \\
&= \eta \left[\left((1 - \overline{p_{a,c}^{(c)}}) \phi_{a,c} - (1 - \overline{p_{b,c}^{(c)}}) (\phi_{a,c} + \Delta_{\phi_c}^{a,b}) \right) - \left(\sum_{\bar{c}} \overline{p_{a,\bar{c}}^{(c)}} \phi_{a,\bar{c}} - \sum_{\bar{c}} \overline{p_{b,\bar{c}}^{(c)}} (\phi_{a,\bar{c}} + \Delta_{\phi_c}^{a,b}) \right) \right] \\
&= \eta \left[\left((\overline{p_{b,c}^{(c)}} - \overline{p_{a,c}^{(c)}}) \phi_{a,c} - (1 - \overline{p_{b,c}^{(c)}}) \Delta_{\phi_c}^{a,b} \right) - \left(\sum_{\bar{c}} (\overline{p_{a,\bar{c}}^{(c)}} - \overline{p_{b,\bar{c}}^{(c)}}) \phi_{a,\bar{c}} - \sum_{\bar{c}} \overline{p_{b,\bar{c}}^{(c)}} \Delta_{\phi_c}^{a,b} \right) \right] \\
&\stackrel{\overline{p_{a,\bar{c}}^{(c)}} = \overline{p_{b,\bar{c}}^{(c)}}}{=} \sum_{\bar{c} \in [C]} \overline{p_{b,\bar{c}}^{(c)}} \Delta_{\phi_c}^{a,b} - \eta \Delta_{\phi_c}^{a,b}.
\end{aligned} \tag{18}$$

Herein, if client a and client b are training their models locally instead of federated training, they can classify the classes they have in local dataset. For further analysis, we assume their possibility outputs for class c are the same, i.e., $\overline{p_{a,\bar{c}}^{(c)}} = \overline{p_{b,\bar{c}}^{(c)}}$.

G.4 PROOF OF THEOREM 3

Assumption 3 With the property of feature anchor loss (3), the feature polymerization in Figures 5 and 7 supports to assume $\bar{\mathbf{h}}_{\cdot,c} = \mathbf{a}_c$ in the following analysis of FedFA. Note that when $\bar{\mathbf{h}}_{\cdot,c} = \mathbf{a}_c$, FedAvg is the same as FedFA without classifier calibration. However, in fact, FedAvg is worse than FedFA without classifier calibration due to feature inconsistency across clients (i.e., $\bar{\mathbf{h}}_{\cdot,c} \neq \mathbf{a}_c$) as denoted by Theorem 2.

For $\mathbf{a}_c = \bar{\mathbf{h}}_{\cdot, y_j}$ when $y_j = c$, we follow (13) and represent the mean prediction output of FedAvg for the c -th class as:

$$\begin{aligned}
\overline{p_{\cdot,c}^{(c)}} &= \frac{1}{n_{\cdot,c}} \sum_{y_j=c}^{n_{\cdot,c}} \hat{p}_{\cdot,c}^{(j)} = \frac{1}{n_{\cdot,c}} \sum_{y_j=c}^{n_{\cdot,c}} \exp(\phi_{\cdot,c}^\top \mathbf{h}_{\cdot,y_j}) / \sum_{q=1}^C \exp(\phi_{\cdot,q}^\top \mathbf{h}_{\cdot,y_j}) \\
&\approx \exp(\phi_{\cdot,c}^\top \bar{\mathbf{h}}_{\cdot,y_j}) / \sum_{q=1}^C \exp(\phi_{\cdot,q}^\top \bar{\mathbf{h}}_{\cdot,y_j}) \\
&= \exp(\phi_{\cdot,c}^\top \mathbf{a}_{\cdot,c}) / \sum_{q=1}^C \exp(\phi_{\cdot,q}^\top \mathbf{a}_{\cdot,c}).
\end{aligned} \tag{19}$$

Similarly, we represent the mean prediction output of FedFA as $\overline{\hat{p}_{\cdot,c}^{(c)}}$,

According to the local classifier calibration, the minimization of (5) for the c -th class can be transformed as:

$$\begin{aligned}
\min_{\phi_{i,c}} \mathcal{L}_{\text{cal}_i}(\phi_{i,c}) &:= \mathbb{E}_{\mathbf{a}_c \in \{\mathbf{a}_c\}_{c=1}^C} [l_{\text{cal}_i}(\phi_{i,c}; (\mathbf{a}_c, c))] \\
&= -\log \frac{\exp(\phi_{i,c}^\top \mathbf{a}_c)}{\sum_{q=1}^C \exp(\phi_{i,q}^\top \mathbf{a}_c)} \\
&= -\overline{\hat{p}_{i,c}^{(c)}} \\
&= \sum_{\bar{c} \in \{[C] \setminus c\}} \overline{\hat{p}_{i,\bar{c}}^{(c)}} - 1.
\end{aligned} \tag{20}$$

Thus, comparing FedFA with FedAvg, for the c -th class prediction output, we have $\overline{\hat{p}_{i,c}^{(c)}} > \overline{p_{i,c}^{(c)}}$ and $\overline{\hat{p}_{i,\bar{c}}^{(c)}} < \overline{p_{i,\bar{c}}^{(c)}}$.

Proof 4 (Proof of Theorem 3) According to the gradient of cross entropy loss, we follow the Definition G.1 and compute the deviation of gradient norms of the global classifier between FedFA and FedAvg as:

$$\begin{aligned}
\|\nabla_{\phi_c} \hat{\mathcal{L}}\|^2 - \|\nabla_{\phi_c} \mathcal{L}\|^2 &= \|\Delta \hat{\phi}_c\|^2 - \|\Delta \phi_c\|^2 = \|\sum_i^N \Delta \hat{\phi}_{i,c}\|^2 - \|\sum_i^N \Delta \phi_{i,c}\|^2 \\
&= \|\frac{\eta}{n} \sum_i^N \left[\left(n_{i,c} (1 - \overline{\hat{p}_{i,c}^{(c)}}) \mathbf{a}_c \right) - \left(\sum_{\bar{c}_i \neq c} n_{i,\bar{c}_i} \overline{\hat{p}_{i,c}^{(\bar{c}_i)}} \mathbf{a}_{\bar{c}_i} \right) \right]\|^2 \\
&\quad - \|\frac{\eta}{n} \sum_i^N \left[\left(n_{i,c} (1 - \overline{p_{i,c}^{(c)}}) \mathbf{a}_c \right) - \left(\sum_{\bar{c}_i \neq c} n_{i,\bar{c}_i} \overline{p_{i,c}^{(\bar{c}_i)}} \mathbf{a}_{\bar{c}_i} \right) \right]\|^2 \\
&= \|\frac{\eta}{n} \left[\underbrace{\sum_i^N \left(n_{i,c} (1 - \overline{\hat{p}_{i,c}^{(c)}}) \right) \mathbf{a}_c}_{\hat{A}_c} - \underbrace{\sum_{\bar{c} \neq c} \sum_i^N n_{i,\bar{c}} \overline{\hat{p}_{i,c}^{(\bar{c})}} \mathbf{a}_{\bar{c}}}_{\hat{B}_{\bar{c}}} \right]\|^2 \\
&\quad - \|\frac{\eta}{n} \left[\underbrace{\sum_i^N \left(n_{i,c} (1 - \overline{p_{i,c}^{(c)}}) \right) \mathbf{a}_c}_{A_c} - \underbrace{\sum_{\bar{c} \neq c} \sum_i^N n_{i,\bar{c}} \overline{p_{i,c}^{(\bar{c})}} \mathbf{a}_{\bar{c}}}_{B_{\bar{c}}} \right]\|^2
\end{aligned} \tag{21}$$

where $\Delta \hat{\phi}_c$ and $\Delta \phi_c$ is the update of the global classifier of FedFA and FedAvg, respectively; $A_c = \sum_i^N \left(n_{i,c} (1 - \overline{p_{i,c}^{(c)}}) \right)$, $\hat{A}_c = \sum_i^N \left(n_{i,c} (1 - \overline{\hat{p}_{i,c}^{(c)}}) \right)$, $B_{\bar{c}} = \sum_i^N n_{i,\bar{c}} \overline{p_{i,c}^{(\bar{c})}}$, $\hat{B}_{\bar{c}} = \sum_i^N n_{i,\bar{c}} \overline{\hat{p}_{i,c}^{(\bar{c})}}$.

Thus, we have:

$$\begin{aligned}
\|\nabla_{\phi_c} \hat{\mathcal{L}}\|^2 - \|\nabla_{\phi_c} \mathcal{L}\|^2 &= \frac{\eta^2}{n^2} \left[\|\hat{A}_c \mathbf{a}_c - \sum_{\bar{c} \neq c} \hat{B}_{\bar{c}} \mathbf{a}_{\bar{c}}\|^2 - \|A_c \mathbf{a}_c - \sum_{\bar{c} \neq c} B_{\bar{c}} \mathbf{a}_{\bar{c}}\|^2 \right] \\
&= \frac{\eta^2}{n^2} [(\hat{A}_c^2 - A_c^2) \|\mathbf{a}_c\|^2 + \sum_{\bar{c} \neq c} (\hat{B}_{\bar{c}}^2 - B_{\bar{c}}^2) \|\mathbf{a}_{\bar{c}}\|^2 \\
&\quad + \sum_{\bar{c}_1 \neq \bar{c}_2} 2(\hat{B}_{c_1} \hat{B}_{c_2} - B_{c_1} B_{c_2}) \mathbf{a}_{\bar{c}_1} \cdot \mathbf{a}_{\bar{c}_2} - \sum_{\bar{c} \neq c} 2(\hat{A}_c \hat{B}_{\bar{c}} - A_c B_{\bar{c}}) \mathbf{a}_c \cdot \mathbf{a}_{\bar{c}}] \\
&\stackrel{\mathbf{a}_c \cdot \mathbf{a}_{\bar{c}} = 0}{=} \frac{\eta^2}{n^2} \left[\underbrace{(\hat{A}_c^2 - A_c^2)}_{less than 0 due to \hat{p}_{i,c}^{(c)} > p_{i,c}^{(c)}} \|\mathbf{a}_c\|^2 + \sum_{\bar{c} \neq c} \underbrace{(\hat{B}_{\bar{c}}^2 - B_{\bar{c}}^2)}_{less than 0 due to \hat{p}_{i,\bar{c}}^{(c)} < p_{i,\bar{c}}^{(c)}} \|\mathbf{a}_{\bar{c}}\|^2 \right] \\
&< 0
\end{aligned} \tag{22}$$

where $\bar{c}_1 \in \{[C] \setminus c\}$, $\bar{c}_2 \in \{[C] \setminus c\}$ and $\bar{c}_1 \neq \bar{c}_2$. Meanwhile, it should be denoted that the assumption $\mathbf{a}_c \cdot \mathbf{a}_{\bar{c}} = 0$ provides an initialization method for feature anchors in FedFA, where more related discussion can be found in Appendix B.2.2.

G.5 PROOF OF THEOREM 4

Proof 5 (Theorem 4) Let $A = \sum_{j_i=1, y_{j_i}=c}^{n_i} \left(1 - p_{j_i,c}^{(i)}\right) \mathbf{h}_{i,y_{j_i}} - \sum_{j_i=1, y_{j_i} \neq c}^{n_i} p_{j_i,c}^{(i)} \mathbf{h}_{i,y_{j_i}}$, and $B = \sum_{j_v=1, y_{j_v}=c}^{n_v} \left(1 - p_{j_v,c}^{(v)}\right) \mathbf{h}_{v,y_{j_v}} - \sum_{j_v=1, y_{j_v} \neq c}^{n_v} p_{j_v,c}^{(v)} \mathbf{h}_{v,y_{j_v}}$.

We compute the similarity of classifier updates between client i and client v ,

$$\cos(\Delta\phi_{i,c}, \Delta\phi_{v,c}) = \frac{\langle \Delta\phi_{i,c}, \Delta\phi_{v,c} \rangle}{\|\Delta\phi_{i,c}\| \|\Delta\phi_{v,c}\|} = \frac{\eta^2 \langle A, B \rangle}{n_i n_v \|A\| \|B\|}. \tag{23}$$

$$\begin{aligned}
\text{Let } A_1 &= \sum_{j_i=1, y_{j_i}=c}^{n_i} \left(1 - p_{j_i,c}^{(i)}\right) \mathbf{h}_{i,y_{j_i}}, \quad A_2 = \sum_{j_i=1, y_{j_i} \neq c}^{n_i} p_{j_i,c}^{(i)} \mathbf{h}_{i,y_{j_i}}, \quad B_1 = \\
&\sum_{j_v=1, y_{j_v}=c}^{n_v} \left(1 - p_{j_v,c}^{(v)}\right) \mathbf{h}_{v,y_{j_v}} \text{ and } B_2 = \sum_{j_v=1, y_{j_v} \neq c}^{n_v} p_{j_v,c}^{(v)} \mathbf{h}_{v,y_{j_v}}.
\end{aligned}$$

Herein, we represent $\langle A, B \rangle$ as:

$$\begin{aligned}
\langle A, B \rangle &= \langle A_1 - A_2, B_1 - B_2 \rangle \\
&= \langle A_1, B_1 \rangle + \langle A_2, B_2 \rangle - \langle A_1, B_2 \rangle - \langle A_2, B_1 \rangle.
\end{aligned} \tag{24}$$

According to Assumption 1, when $\mathbf{h}_c \in \mathcal{H}_c$ and $\mathbf{h}_q \in \mathcal{H}_q$ and $c \neq q$, the inner product $\langle \mathbf{h}_c, \mathbf{h}_q \rangle$ is less than or equal to 0. Thus, we have:

$$\begin{aligned}
\langle A_1, B_2 \rangle &= \left\langle \sum_{j_i=1, y_{j_i}=c}^{n_i} \left(1 - p_{j_i,c}^{(i)}\right) \mathbf{h}_{i,y_{j_i}}, \sum_{j_v=1, y_{j_v} \neq c}^{n_v} p_{j_v,c}^{(v)} \mathbf{h}_{v,y_{j_v}} \right\rangle \\
&= \sum_{j_v=1, y_{j_v} \neq c}^{n_v} \sum_{j_i=1, y_{j_i}=c}^{n_i} \left(1 - p_{j_i,c}^{(i)}\right) p_{j_v,c}^{(v)} \langle \mathbf{h}_{i,y_{j_i}}, \mathbf{h}_{v,y_{j_v}} \rangle \\
&\leq 0
\end{aligned} \tag{25}$$

where the inequality holds because $y_{j_i} = c$ but $y_{j_v} \neq c$ and thus $\langle \mathbf{h}_{i,y_{j_i}}, \mathbf{h}_{v,y_{j_v}} \rangle \leq 0$.

Similarly, we have:

$$\begin{aligned}
\langle A_2, B_1 \rangle &= \left\langle \sum_{j_i=1, y_{j_i} \neq c}^{n_i} p_{j_i,c}^{(i)} \mathbf{h}_{i,y_{j_i}}, \sum_{j_v=1, y_{j_v}=c}^{n_v} \left(1 - p_{j_v,c}^{(v)}\right) \mathbf{h}_{v,y_{j_v}} \right\rangle \\
&\leq 0.
\end{aligned} \tag{26}$$

Also, according to Assumption 1, when $\|\mathbf{a}_c\| > \sqrt{2}\delta$, for any $\mathbf{h}_{i,c} \in \mathcal{H}_c$ and $\mathbf{h}_{v,c} \in \mathcal{H}_c$, we obtain that the inner product $\langle \mathbf{h}_{i,c}, \mathbf{h}_{v,c} \rangle$ is larger than 0 since the arccosine of largest angle between $\mathbf{h}_{i,c}$ and $\mathbf{h}_{v,c}$ is $2\arccos(\|\mathbf{a}_c\|/\sqrt{2}\delta)$ (i.e., the largest angle is smaller than $\pi/2$).

$$\begin{aligned}
\langle A_1, B_1 \rangle &= \left\langle \sum_{j_i=1, y_{j_i}=c}^{n_i} \left(1 - p_{j_i, c}^{(i)}\right) \mathbf{h}_{i, y_{j_i}}, \sum_{j_v=1, y_{j_v}=c}^{n_v} \left(1 - p_{j_v, c}^{(v)}\right) \mathbf{h}_{v, y_{j_v}} \right\rangle \\
&= \sum_{j_v=1, y_{j_v}=c}^{n_v} \sum_{j_i=1, y_{j_i}=c}^{n_i} \left(1 - p_{j_i, c}^{(i)}\right) \left(1 - p_{j_v, c}^{(v)}\right) \langle \mathbf{h}_{i, y_{j_i}}, \mathbf{h}_{v, y_{j_v}} \rangle \\
&> 0.
\end{aligned} \tag{27}$$

Similarly, we have:

$$\begin{aligned}
\langle A_2, B_2 \rangle &= \left\langle \sum_{j_i=1, y_{j_i} \neq c}^{n_i} p_{j_i, c}^{(i)} \mathbf{h}_{i, y_{j_i}}, \sum_{j_v=1, y_{j_v} \neq c}^{n_v} p_{j_v, c}^{(v)} \mathbf{h}_{v, y_{j_v}} \right\rangle \\
&> 0.
\end{aligned} \tag{28}$$

Combining (24) to (28), we obtain that $\langle A, B \rangle$ is larger than 0, and thus $\cos(\Delta\phi_{i,c}, \Delta\phi_{v,c}) > 0$.